Author/s:
Soh, MS;Hu, A;Kuanyshbek, A;Mohamed Syazwan, ES;Lee, HM;McKenzie, CE;Phillips, AM;Bleakley, LE;Semsarian, C;Scheffer, IE;Berkovic, SF;Reid, CA

Title:
Atenolol rescues premature mortality in genetic mouse models of sudden unexpected death in epilepsy

Date:
2026-01-01

Citation:
Soh, M. S., Hu, A., Kuanyshbek, A., Mohamed Syazwan, E. S., Lee, H. M., McKenzie, C. E., Phillips, A. M., Bleakley, L. E., Semsarian, C., Scheffer, I. E., Berkovic, S. F. & Reid, C. A. (2026). Atenolol rescues premature mortality in genetic mouse models of sudden unexpected death in epilepsy. Epilepsia, 67 (1), pp.448-462. https://doi.org/10.1111/epi.18642.

Atenolol rescues premature mortality in genetic mouse models of sudden unexpected death in epilepsy.

Ming S. Soh[1], Amanda Hu[1], Alibek Kuanyshbek[1], Erlina S. Mohamed Syazwan[1], Hian M. Lee[1], Chaseley E. McKenzie[1], A. Marie Phillips[1,2], Lauren E. Bleakley[1], Christopher Semsarian[3,4,5], Ingrid E. Scheffer[1,6,7,8], Samuel F. Berkovic[6], Christopher A. Reid[1]

Author affiliations:

[1]The Florey Institute of Neuroscience and Mental Health, University of Melbourne, Parkville, VIC, Australia

[2]School of Biosciences, University of Melbourne, Melbourne, VIC, Australia

[3]Agnes Ginges Centre for Molecular Cardiology at Centenary Institute, The University of Sydney, Sydney, NSW, Australia

[4]Faculty of Medicine and Health, The University of Sydney, NSW, Australia

[5]Department of Cardiology, Royal Prince Alfred Hospital, Sydney, NSW, Australia

[6]Epilepsy Research Centre, Department of Medicine, University of Melbourne, Austin Health, Heidelberg, VIC, Australia

[7]Murdoch Children's Research Institute, The Royal Children's Hospital, Parkville, VIC, Australia

[8]Department of Paediatrics, University of Melbourne, Royal Children's Hospital, VIC, Australia

Correspondence:

Christopher A. Reid

Address: The Florey Institute of Neuroscience and Mental Health, University of Melbourne,

30 Royal Parade, Parkville 3052, Victoria, Australia

Email: christopher.reid@florey.edu.au

Contact: +61 3 9035 6372

ORCID: 0000-0002-1457-8028

Number of text pages: 21

Number of words: 4,166

Number of references: 49

Number of figures: 6

Number of tables: 0

Abstract

Objective: Sudden Unexpected Death in Epilepsy (SUDEP) is the leading cause of premature mortality in epilepsy. Genetic studies have identified that loss-of-function (LOF) *KCNH2* variants are enriched in SUDEP patients suggesting that they may act as a risk factor. *KCNH2* encodes the $K_V11.1$ channel with LOF pathogenic variants a cause of long-QT syndrome (LQTS), increasing the risk of arrhythmia and sudden cardiac death. Here, we engineered preclinical rodent models that combine epilepsy-causing pathogenic variants with heterozygous *Kcnh2* knockout mice to explore the impact of reduced $K_V11.1$ channel function on mortality.

Methods: Both the *Gabrg2*$^{R43Q/+}$ and *Hcn1*$^{M294L/+}$ genetic mouse models of monogenic epilepsy were crossed with *Kcnh2*$^{+/-}$ mice. All genotypes were video-recorded post-weaning and time to death was measured. Additional mice underwent surgery to enable simultaneous electrocorticography and electrocardiography recordings. Atenolol was delivered in drinking water to a subset of mice.

Results: Both single mutant *Gabrg2*$^{R43Q/+}$ and *Hcn1*$^{M294L/+}$ mice displayed spontaneous seizures recapitulating the human phenotypes. Single mutant *Kcnh2*$^{+/-}$ mice exhibited a LQTS phenotype. Double mutant mice (*Gabrg2*$^{R43Q/+}$/*Kcnh2*$^{+/-}$ and *Hcn1*$^{M294L/+}$/*Kcnh2*$^{+/-}$) had both seizure and prolonged QT interval phenotypes that were similar to their respective single mutant mice. Survival analysis revealed that *Gabrg2*$^{R43Q/+}$/*Kcnh2*$^{+/-}$ and *Hcn1*$^{M294L/+}$/*Kcnh2*$^{+/-}$ mice experienced a disproportionately higher rate of seizure-related death when compared to wild-type and their respective single mutant littermates. Oral administration of the cardiac-selective β-blocker atenolol significantly improved survival in *Gabrg2*$^{R43Q/+}$/*Kcnh2*$^{+/-}$, *Hcn1*$^{M294L/+}$, and *Hcn1*$^{M294L/+}$/*Kcnh2*$^{+/-}$ mice. Atenolol attenuated the sympathetic cardiac response to non-terminal seizures.

Significance: The data support the premise that loss-of-function *KCNH2* variants can contribute to SUDEP risk in a subset of epilepsy patients. Our findings also highlight the potential use of β-blockers as a prevention strategy in SUDEP.

Keywords: SUDEP; cardiac arrhythmia; *KCNH2*; atenolol; long-QT syndrome

Key Points

- Loss of $K_V11.1$ channel function increases the risk of seizure-mediated premature death in genetic models of epilepsy.
- Loss-of-function $K_V11.1$ did not alter seizure susceptibility in the *Gabrg2* and *Hcn1* genetic epilepsy mouse models.
- Loss of $K_V11.1$ channel function induced a prolonged QT interval that models long-QT syndrome type 2.
- The β-blocker atenolol improved survival in both genetic mouse models of SUDEP.
- Atenolol reduced heart rate and QTc interval, without affecting seizure load in both mouse models of SUDEP.

Introduction

Sudden unexpected death in epilepsy (SUDEP) is the most common cause of premature mortality for the estimated 50 million people with epilepsy globally.[1] The International League Against Epilepsy defines SUDEP as a sudden, unexpected death in a person with epilepsy, with or without evidence for a seizure preceding the death, in which there is no evidence of other disease, injury, or drowning that caused the death.[2, 3] SUDEP often occurs among young adults and is second only to stroke in years of potential life lost among neurological diseases, making it the most catastrophic complication of epilepsy.[4] As most cases are not witnessed at the time of death, it remains a challenge to dissect the exact cause underlying SUDEP. There are several recognised SUDEP risk factors including frequent generalised tonic-clonic seizures, poor treatment adherence, and resistance to anti-seizure medications.[5, 6] Nonetheless, patients with well-controlled seizures can still experience SUDEP.[5, 6] The involvement of neuro-cardio-respiratory pathways is hypothesised to be the primary cause of death in SUDEP.[7, 8] In the Mortality in Epilepsy Monitoring Unit Study (MORTEMUS), 67% of the studied SUDEP cases experienced terminal apnoea prior to terminal asystole, suggesting seizure-induced respiratory depression as a key contributor to cardiorespiratory failure.[9] This then led to a proposed unifying hypothesis of SUDEP based on seizure-induced respiratory depression.[10] However, the mechanism is more complex, as the remaining 33% of cases in the MORTEMUS study indicated that terminal events were preceded by cardiorespiratory dysfunction. Furthermore, significant cardiac events including bradycardia and transient asystole preceded terminal apnoea in most patients.[9, 11] It is therefore likely that the underlying cause of SUDEP is complex, multifactorial and may vary between patients.

Cardiac arrhythmia has been regularly proposed as one of the possible causes of SUDEP.[12] One reason relates to the similarities between SUDEP and sudden cardiac death due to arrhythmias.[13] Furthermore, changes in cardiac function consistent with sympathetic

overactivity, including an increase in heart rate and life-threatening arrhythmia, can occur during epileptic seizures.[14-16] Recently, a retrospective study demonstrated that prolonged QT interval on the electrocardiogram (ECG) could predict all-cause mortality in patients with epilepsy.[17] In two other retrospective studies, lower heart rate variability was found to be associated with a higher SUDEP risk.[18, 19] With increased genetic testing in recent years, pathogenic variants in major cardiac genes such as *KCNH2* and *SCN5A*, which can cause inherited arrhythmia syndromes, have been identified in up to 15% of SUDEP cases.[7, 20-22] Pathogenic *KCNH2* variants, in particular, were most frequently implicated in a large genetic analysis of SUDEP patients.[20]

KCNH2, also known as the human Ether-à-go-go-Related Gene or hERG, encodes the potassium ion channel $K_v11.1$, which is expressed widely in the heart and brain.[13] In the heart, this channel is responsible for regulating the delayed rectifier potassium current, I_{kr}, critical for phase 3 repolarisation following a cardiac action potential. Loss-of-function pathogenic *KCNH2* variants cause a congenital arrhythmia condition known as long-QT syndrome (LQTS).[13] One of the characteristics of LQTS is the prolongation of the QT interval on the ECG that increases the risk of a severe form of ventricular arrhythmia known as 'torsades de pointes', which in turn can trigger sudden cardiac death.[13, 23] LQTS2 caused by loss-of-function *KCNH2* variants accounts for approximately 30% of all LQTS cases.[13] In the brain, $K_v11.1$ regulates neuronal excitability and has been associated with epileptiform discharges, seizures and epilepsy.[24-29] However, as patients with LQTS often experience syncope accompanied by seizure-like movements, possibly due to cerebral hypoperfusion, some are misdiagnosed with epilepsy and incorrectly treated with anti-seizure medications.[24, 30]

Our recent study found a 3-fold enrichment of *KCNH2* variants that caused a loss of $K_v11.1$ function in individuals who experienced SUDEP compared with living epilepsy

patients.[31] This suggests that loss-of-function *KCNH2* variants can increase SUDEP risk. We hypothesised that the increased risk of sudden death is due to the combined effects of seizure- and LQTS-mediated cardiac dysfunction. Furthermore, we postulated that repurposing a LQTS treatment could decrease the risk of SUDEP. To test this, we developed two novel SUDEP mouse models that have both genetic epilepsy and *Kcnh2*-mediated LQTS. Our results demonstrated that loss-of-function *Kcnh2* significantly reduced survival in both mouse models of epilepsies without affecting seizure susceptibility. Importantly, oral treatment with the relatively cardiac-selective β-blocker, atenolol, was able to rescue both SUDEP mouse models from premature death.

Materials and methods

Animal ethics approval

All animal procedures comply with the institutional and national guide for the care and use of laboratory animals, as outlined in Supplementary Materials and Methods (Appendix S1).

Animal model

Generation of the single mutant, heterozygous *Gabrg2*$^{R43Q/+}$, *Hcn1*$^{M294L/+}$ and *Kcnh2*$^{+/-}$ mice were previously outlined.[32-35] See Appendix S1 for maintenance and housing details.

Survival recording and treatment study

Once weaned, the mice were brought to an experimental room where they were weighed and group-housed according to sex and genotype. Video recording (SANNCE, Rowland Heights, CA, USA) then commenced until P100 (Appendix S1).

For treatment study, only the double mutant mice (*Gabrg2*$^{R43Q/+}$/*Kcnh2*$^{+/-}$, *Hcn1*$^{M294L/+}$/*Kcnh2*$^{+/-}$) were video-recorded according to the same protocol as above. At P21 (weaning age, for *Hcn1*$^{M294L/+}$ and *Hcn1*$^{M294L/+}$/*Kcnh2*$^{+/-}$) or P40, (for *Gabrg2*$^{R43Q/+}$/*Kcnh2*$^{+/-}$), mice were randomly given normal or atenolol-dissolved (Cayman Chemical, Ann Arbor, MI, USA) tap drinking water.

Implantation of electrocorticography and electrocardiography electrodes

Instrumentation of electrocorticography (ECoG) and electrocardiography (ECG) electrodes were performed on mice aged >P25, as outlined in Appendix S1.

Electrocorticography and electrocardiography recording

The head mount was connected to a preamplifier with 10x amplification (Pinnacle Technology Inc., Lawrence, KS, USA), which in turn was connected to a data acquisition system (Sirenia 2.1.0, Pinnacle Technology Inc., Lawrence, KS, USA) (Appendix S1). Recordings were sampled at a rate of 2 kHz, allowing for robust measurements of QT intervals.

Baseline epileptiform analysis

The entire 24-hour ECoG recording was visually analysed for spikes, spike-wave discharges (SWDs) and seizures using Sirenia software (version 2.1.0, Pinnacle Technology Inc., Lawrence, KS, USA), detailed in Appendix S1.

Analysis of cardiac parameters

ECG parameters were exported using Sirenia software and analysis outlined in Appendix S1. QTc interval was calculated using the Mitchell's formula, which was based on the Bazett's formula modified for mice; $QTc = \frac{QT}{\sqrt{RR/100}}$.[36]

Heart rate variability (HRV) was calculated based on Root Mean Square of the Successive Differences (RMSSD) formula; $HRV = \sqrt{\frac{\sum_{i=1}^{N-1}(RR_i - RR_{i+1})^2}{N-1}}$.

Statistical analyses

All statistical analyses were performed using GraphPad Prism software (version 9.2.0, Boston, MA, USA). Survival curves were plotted with Kaplan-Meier estimator and analysed using Mantel-Cox log-rank test. All other data were reported as mean ± standard error of the mean (SEM). Data sets were first analysed using a Shapiro-Wilk test for normality. For statistical comparison of two normally distributed data sets, an unpaired two-tailed Student's *t*-test was used. For data set where Shapiro-Wilk test returned $P < 0.05$, a Mann-Whitney U-test was used

for two-group comparison. One-way ANOVA with Dunnett's post-hoc or Kruskal-Wallis with Dunn's test was used for statistical comparison of more than two normally or non-normally distributed data groups respectively. Welch's correction test was used for groups with unequal variances. Mixed model analysis with Tukey's post-hoc was used for groups with repeated measurements. Statistical significance was set at $P < 0.05$.

Results

To develop the first genetic combination model of SUDEP, *Gabrg2*$^{R43Q/+}$ and *Kcnh2*$^{+/-}$ mice were crossed to produce a double mutant model. The *Gabrg2*$^{R43Q/+}$ mouse is a well-established model of generalised epilepsy based on a pathogenic arginine to glutamine variant at position 43 in $GABA_A$ γ2 subunit gene *GABRG2*.[34, 37] *Kcnh2*$^{+/-}$ mice have loss-of-function *Kcnh2* and model LQTS.[33, 35] Mating between *Gabrg2*$^{R43Q/+}$ and *Kcnh2*$^{+/-}$ mice produced littermates which were born in Mendelian ratio of the four genotypes (wild-type, *Gabrg2*$^{R43Q/+}$, *Kcnh2*$^{+/-}$, *Gabrg2*$^{R43Q/+}$/*Kcnh2*$^{+/-}$). All mice appeared healthy with weights of the littermates similar across age for the different genotypes (Figure S1; Table S1).

Heterozygous *Kcnh2* knockout does not alter seizure phenotypes in *Gabrg2*$^{R43Q/+}$ mice

We first characterised the baseline epileptiform activity of littermates of the four genotypes through 24-hour video electrocorticography (ECoG) recording (Figure 1A–G and Table S1). We confirmed that the *Gabrg2*$^{R43Q/+}$ mice recapitulated generalised epilepsy features seen in humans, including interictal spiking (Figure 1B and C) and spike-and-wave discharges (SWDs) (Figure 1D and E).[34, 37] A subset of *Gabrg2*$^{R43Q/+}$ mice also experienced spontaneous Racine 2-3 seizures with nodding, forelimb clonus, rearing and/or extended tail (Figure 1F and G). Double mutant *Gabrg2*$^{R43Q/+}$/*Kcnh2*$^{+/-}$ mice also exhibited interictal spiking, SWDs and rare spontaneous Racine 2-4 class seizures (Figure 1B–G). Importantly, comparison of the seizure phenotype between *Gabrg2*$^{R43Q/+}$ and *Gabrg2*$^{R43Q/+}$/*Kcnh2*$^{+/-}$ mice revealed no differences in the frequencies of interictal spikes, SWDs or spontaneous seizures (Figure 1B–G). As expected, ECoG recording revealed no spontaneous seizures and only a minimal number of interictal spikes and SWDs in the wild-type and single mutant *Kcnh2*$^{+/-}$ mice (Figure 1A–G; Table S1). These data suggest that heterozygous knockout of *Kcnh2* does not modulate epileptiform or spontaneous seizure activity in the *Gabrg2*$^{R43Q/+}$ mouse model.

Prolonged QT interval occurs in *Kcnh2*$^{+/-}$ and *Gabrg2*$^{R43Q/+}$/*Kcnh2*$^{+/-}$ mice

24-hour video-ECG recordings were made to measure cardiac parameters in littermates of the *Gabrg2*$^{R43Q/+}$ and *Kcnh2*$^{+/-}$ mating (Figure 2). Recordings revealed no spontaneous arrhythmias in either the single *Kcnh2*$^{+/-}$ nor double mutant mice during this period. However, a prolonged corrected QT interval (QTc) was observed in the *Kcnh2*$^{+/-}$ mice compared to wild-type mice, confirming a LQTS phenotype (Figure 2A and B).[33, 35] QTc intervals did not differ between *Gabrg2*$^{R43Q/+}$ and WT mice (Figure 2A and B). *Gabrg2*$^{R43Q/+}$/*Kcnh2*$^{+/-}$ mice also have a prolonged QTc interval that is similar to the *Kcnh2*$^{+/-}$ mice suggesting that the LQTS phenotype is maintained in the double mutant mice (Figure 2A and B). There was no difference in the heart rate variability, RR interval, P-wave duration, or PR interval between the four genotypes (Figure 2C and D, Table S1). Heart weight to body weight ratio was also similar between all groups (Table S1, Appendix 1).

Loss of *Kcnh2* function increases rate of seizure-induced premature death in *Gabrg2*$^{R43Q/+}$ genetic epilepsy mice

To evaluate the impact of having both genetic epilepsy and LQTS on SUDEP risk, we performed long-term 24/7 video recordings on littermates from weaning (P21-P23) until P100. We scored the time of death and evaluated the associated behaviour, including spontaneous seizures (Video S1), shortly before and during death. All wild-type mice survived until the end of the long-term recording at P100 (Figure 3A). A small number of *Kcnh2*$^{+/-}$ (2 out of 37) and *Gabrg2*$^{R43Q/+}$ (4 out of 41) mice died prematurely during the recording period. An increase in spontaneous death rate in the *Gabrg2*$^{R43Q/+}$ single mutant mice is consistent with epilepsy-causing variants independently increasing the risk of premature death.

Strikingly, the double mutant *Gabrg2*$^{R43Q/+}$/*Kcnh2*$^{+/-}$ mice were disproportionately more likely to die prematurely within the timeframe (16 out of 38, Figure 3A), suggesting a

synergistic impact of the two independent risk factors. Both the *Gabrg2*$^{R43Q/+}$ and *Gabrg2*$^{R43Q/+}$/*Kcnh2*$^{+/-}$ mice were all found dead with hind-limb extension. Video recordings confirmed that the mice experienced Racine class 4-5 seizures resulting in death (Video S2). In contrast, the deceased *Kcnh2*$^{+/-}$ single mutant mice did not exhibit hind-limb extension nor were seizures observed prior to death. As seizure characteristics including seizure frequency did not differ in *Kcnh2*$^{+/-}$, this suggests that changes in brain hyperexcitability are unlikely to contribute to the heightened risk of premature death observed in the *Gabrg2*$^{R43Q/+}$/*Kcnh2*$^{+/-}$ mice.

Atenolol improves survival in *Gabrg2*$^{R43Q/+}$/*Kcnh2*$^{+/-}$ mice

β-blockers are first-line therapy for patients with LQTS caused by loss-of-function *KCNH2* variants and are effective in reducing the risk of sudden cardiac death.[38] We therefore hypothesised that repurposing β-blockers may reduce the risk of premature death in our preclinical model of SUDEP. Specifically, we used the relatively cardiac-selective blocker, atenolol, which has a higher affinity for the β_1-adrenergic receptor and does not cross the blood-brain barrier.[39] We randomly assigned *Gabrg2*$^{R43Q/+}$/*Kcnh2*$^{+/-}$ mice to either atenolol-treated or untreated group. In the atenolol-treated groups, we dissolved 0.1 or 0.6 g/L atenolol in tap drinking water and introduced the treatment from P40. The time point P40 was chosen as this was before the first death was recorded in the *Gabrg2*$^{R43Q/+}$/*Kcnh2*$^{+/-}$ mice (Figure 3A). Untreated mice were given standard tap drinking water. The average volume drunk was similar between untreated and atenolol-treated groups (Figure S2) and neither dose of drug caused any overt behavioural changes in the mice. A low atenolol dose (0.1 g/L) was ineffective at improving survival (Figure 3B). Strikingly, a higher 0.6 g/L atenolol dose significantly improved survival in the *Gabrg2*$^{R43Q/+}$/*Kcnh2*$^{+/-}$ double mutant mice (Figure 3B).

Impact of atenolol on seizure and cardiac phenotypes in *Gabrg2*$^{R43Q/+}$/*Kcnh2*$^{+/-}$ mice

ECG recordings performed on untreated and 0.6 g/L atenolol-treated *Gabrg2*$^{R43Q/+}$/*Kcnh2*$^{+/-}$ mice revealed that atenolol significantly reduced the QTc interval (Figure S3A and B). Atenolol prolonged the RR interval considerably by about 15.5 ms (Figure S3C), equivalent to a reduction in heart rate of approximately 15% which is consistent with reductions seen in humans at therapeutic doses of atenolol.[40] Atenolol also increased RMSSD, but had no impact on P-wave duration or PR interval (Figure S3D, Table S2).

To test if 0.6 g/L atenolol impacted seizure load, ECoG recordings were performed on untreated and atenolol-treated *Gabrg2*$^{R43Q/+}$/*Kcnh2*$^{+/-}$ mice (Figure S4 and Table S2). As expected, atenolol had no impact on interictal spiking (Figure S4A and B), SWDs (Figure S4C and D), or spontaneous seizures (Figure S4E and F) in the *Gabrg2*$^{R43Q/+}$/*Kcnh2*$^{+/-}$ mice (Table S2).

Increased rate of seizure-induced premature death in *Hcn1*$^{M294L/+}$ and *Hcn1*$^{M294L/+}$/*Kcnh2*$^{+/-}$ mice is also reversed by atenolol

To investigate if loss of *Kcnh2* function increases the risk of premature death in a different genetic epilepsy mouse model, the *Kcnh2*$^{+/-}$ mouse was crossed with the well-characterised *Hcn1*$^{M294L/+}$ mouse model of *HCN1* developmental and epileptic encephalopathy (DEE).[32] The littermates were born with approximate Mendelian ratio of four genotypes: wild-type, *Hcn1*$^{M294L/+}$, *Kcnh2*$^{+/-}$, or *Hcn1*$^{M294L/+}$/*Kcnh2*$^{+/-}$. Both *Hcn1*$^{M294L/+}$ and *Hcn1*$^{M294L/+}$/*Kcnh2*$^{+/-}$ mice were born of smaller size compared to wild-type and *Kcnh2*$^{+/-}$ mice (Figure S1 and Table S3).[32]

Hcn1$^{M294L/+}$ and *Hcn1*$^{M294L/+}$/*Kcnh2*$^{+/-}$ mice experienced similar, and significantly higher than wild-type, levels of interictal spiking, SWDs, and spontaneous seizures on the ECoG. This recapitulated previous findings and human phenotypes (Figure 4A-C, Table S3).[32]

Both *Kcnh2*$^{+/-}$ and *Hcn1*$^{M294L/+}$/*Kcnh2*$^{+/-}$ mice displayed prolonged QTc interval at baseline (Figure 4D and E, Table S3). The mice with the *Hcn1*^{M294L} mutation, which is also expressed in the heart, had longer baseline QTc interval than wild-type mice, but not as prolonged as the *Kcnh2*$^{+/-}$ or *Hcn1*$^{M294L/+}$/*Kcnh2*$^{+/-}$ mice (Figure 4E, Table S3). Both *Hcn1*$^{M294L/+}$ and *Hcn1*$^{M294L/+}$/*Kcnh2*$^{+/-}$ mice had shorter RR interval compared to wild-type mice (Figure 4F, Table S3). Heart rate variability was also found to be lower in *Hcn1*$^{M294L/+}$ and *Hcn1*$^{M294L/+}$/*Kcnh2*$^{+/-}$ mice (Table S3). All ECoG and ECG parameters are listed in Table S3. In summary, the double mutant *Hcn1*$^{M294L/+}$/*Kcnh2*$^{+/-}$ mice displayed seizure and LQTS phenotypes that were similar to the respective *Hcn1*$^{M294L/+}$ and *Kcnh2*$^{+/-}$ single mutant mice.

To assess survival, long-term 24/7 video recordings until P100 were performed in littermates of all four genotypes from the cross between *Hcn1*$^{M294L/+}$ and *Kcnh2*$^{+/-}$ mice. No deaths were reported for either wild-type or *Kcnh2*$^{+/-}$ mice during the recorded period (Figure 5A). 25% (6 out of 24) of the single mutant *Hcn1*$^{M294L/+}$ mice died prematurely (Figure 5A). Similarly to that observed for the *Gabrg2*$^{R43Q/+}$/*Kcnh2*$^{+/-}$ mouse model, *Hcn1*$^{M294L/+}$/*Kcnh2*$^{+/-}$ mice were ~2.5-fold more likely to die prematurely when compared to the single mutant *Hcn1*$^{M294L/+}$ mice (Figure 5A). Video recordings revealed that the deaths occurred following a Racine 4-5 seizure in both the single and double mutant mice (Video S3). Importantly, atenolol (0.6 g/L in drinking water) significantly reduced the occurrence of premature death in the *Hcn1*$^{M294L/+}$/*Kcnh2*$^{+/-}$ mice by approximately 40% without impacting brain hyperexcitability (Figure 5B, Table S4). Interestingly, atenolol also improved survival in the single mutant *Hcn1*$^{M294L/+}$ mice (Figure 5C), suggesting that its protective effects extend beyond the increased risk conferred by *Kcnh2*$^{+/-}$. The volume of vehicle or atenolol drunk was similar between the respective groups (Figure S2B and S2C). Our findings in the *Hcn1*$^{M294L/+}$/*Kcnh2*$^{+/-}$ model again support the premise that loss-of-function *Kcnh2* underlies an increased risk of mortality in

epilepsy, and that β-blockers may be a promising therapeutic intervention to reduce SUDEP risk.

Changes in autonomic nervous system activity in the heart during spontaneous seizures

We next compared the effects of spontaneous seizures on ECG parameters in untreated and atenolol-treated *Hcn1*$^{M294L/+}$/*Kcnh2*$^{+/-}$ mice. These seizures were generally Racine 2-3, characterised by rhythmic nodding, forelimb clonus and/or tail extension (Video S4).[41] During seizures, both groups exhibited a significant increase in heart rate and QTc interval, accompanied by a reduction in heart rate variability, relative to their respective baselines (Figure 6A-C, Table S4). This is consistent with seizures causing changes in autonomic drive to the heart.[42] At baseline, atenolol-treated mice showed a shorter QTc interval and longer RR interval and RMSSD compared to untreated mice. While increases in the QTc interval and shorter RR intervals were observed in atenolol-treated mice during seizures, these changes did not reach the maximum extent observed in the untreated mice (Figure 6B and C). These data show that atenolol can partially protect the heart from seizure-mediated autonomic impact, which may account for its ability to reduce premature death in our mouse models. Additionally, arrhythmias, in particular variable AV block with irregular dropping of QRS complexes, were noted, albeit rarely (in 3 double mutant mice), during seizure events (Figure S5A). Out of the three, two were untreated while one was atenolol-treated. One *Hcn1*$^{M294L/+}$/*Kcnh2*$^{+/-}$ mouse was also noted having bradyarrhythmia with AV block at baseline (Figure S5B). The impact of atenolol on the cardiac parameters are presented in Table S4.

During ECoG-ECG recording, one *Hcn1*$^{M294L/+}$/*Kcnh2*$^{+/-}$ mouse experienced hind-limb extension following a spontaneous terminal Racine 4-5 seizure (Figure S6). Capturing clear ECG signals during terminal seizures is technically challenging due to electromyographic noise. However, in this case, a small window occurred where the signal-to-noise dramatically

improved, allowing for clearer ECG interpretation. During this time, we observed arrhythmias, including bradycardia with variable AV block, indicating the possibility of cardiac dysfunction contributing to sudden death (Figure S6).

Discussion

SUDEP is a rare but catastrophic outcome for patients with epilepsy with no clear preventative strategy except improved seizure control. We showed that loss of *Kcnh2* function increased the risk of premature death in a mouse model of *GABRG2* generalised epilepsy and a mouse model of *HCN1* DEE. This is consistent with our previously published human data which demonstrated a 3-fold enrichment of loss-of-function *KCNH2* variants in SUDEP patients compared to a control group living with epilepsy.[31] Collectively, these data support the view that patients with epilepsy carrying loss-of-function *KCNH2* variants are at higher risk of SUDEP. Furthermore, our findings demonstrate that the β-blocker atenolol protects both double mutant mouse models from seizure-induced premature death. Importantly, atenolol's protective effect also extends to the single-mutant *HCN1* DEE mouse model, suggesting potential benefits beyond patients with loss-of-function *KCNH2*. Overall, our data suggest that cardio-protective preventative treatments may be effective at reducing SUDEP risk in a subset of epilepsy patients.

Spontaneous seizures caused an increase in heart rate and prolonged QTc intervals in our *Hcn1*$^{M294L/+}$/*Kcnh2*$^{+/-}$ mouse model, indicating changes in autonomic nervous system activity. Similarly, in humans, tonic-clonic seizures can also lead to a change in autonomic response.[14, 42] Importantly, such changes, especially increased sympathetic activity caused by external stress factors, are well-established triggers of sudden cardiac death in LQTS, suggesting a mechanistic parallel with SUDEP.[43] Seizure-induced sympathetic activation is therefore well-positioned to act as a potential trigger for life-threatening arrhythmias in at-risk individuals. β-blockers are the first-line preventative treatment for LQTS2.[38] Here, we show that atenolol effectively reduced premature death in both our double mutant and single mutant *HCN1* DEE mouse models. By blocking β_1-adrenergic receptors, atenolol reduces sympathetic activity to the heart, causing a reduction in heart rate and shortening of QT intervals.[44] While the atenolol-treated mice still experienced seizure-induced changes in heart rate and QTc, these

effects were less pronounced than in untreated mice. Notably, atenolol reduced premature mortality in our mouse models without influencing seizure susceptibility. This is not unexpected, as atenolol is relatively β_1-cardiac-selective and is thought not to cross the blood-brain barrier,[39] which is not compromised in the *Gabrg2* epilepsy mouse model.[45] Our data strongly support the premise that atenolol reduces premature mortality in mice through a cardio-protective mechanism.

Although previous studies have shown that pathogenic arrhythmia variants, particularly loss-of-function *KCNH2*, are enriched in SUDEP patients,[20, 31] it remains unclear whether pathogenic variants associated with epilepsy and cardiac arrhythmia co-occur in SUDEP patients. Our study using the double mutant models provides important evidence that pathogenic LQTS2 variants can increase mortality risk in the context of monogenic epilepsy. These findings may be relevant to SUDEP more broadly, highlighting the potential contribution of cardiac arrhythmia variants as contributors to SUDEP risk. Wider implementation of genetic screening in patients with epilepsy has provided an opportunity to identify pathogenic variants linked to inherited arrhythmias. An array of different arrhythmia-causing genes should therefore be considered in future SUDEP studies.[7, 20] For example, rare variants in *SCN5A* that affect the cardiac voltage-dependent sodium channel $Na_v1.5$ have been found in SUDEP cases.[21, 46] Concepts developed here could potentially extend to other causes of epilepsy, including those that do not have a genetic origin. Further retrospective and prospective clinical studies are needed to identify epilepsy patients with arrhythmia-related variants, who may be at higher risk of SUDEP, for early intervention.

Case reports and correlative studies have suggested an association between *KCNH2* variants and epilepsy.[24, 25, 27-29, 47] However, the relationship between *KCNH2* variants and seizures is complex. For instance, patients with $K_v11.1$ dysfunction can exhibit syncope

accompanied by seizure-like motor activity, leading to frequent misdiagnosis of epilepsy.[24, 27, 30] Conversely, a significant proportion of LQTS2 individuals exhibit epileptiform activity on the electroencephalograms and are more prone to seizures.[27-29] In our study, the *Kcnh2*$^{+/-}$ mice did not exhibit spontaneous seizures, epileptiform activity, or a significant increase in premature mortality. Furthermore, loss of *Kcnh2* function did not alter spontaneous seizure susceptibility or epileptiform activity in the *Gabrg2*$^{R43Q/+}$/*Kcnh2*$^{+/-}$ and *Hcn1*$^{M294L/+}$/*Kcnh2*$^{+/-}$ mouse models. These findings contrast with a recent study using a knock-in LQTS2 rabbit model, which demonstrated that loss-of-function *Kcnh2* led to increased epileptiform activity, spontaneous seizures and mortality.[48] Collectively, these data indicate that while there is a link between K_v11.1 and epilepsy, it is unlikely to be a key driver of seizures in our mouse models. Nonetheless, *KCNH2* variants may act as genetic modifiers under certain circumstances. Future preclinical and clinical studies are needed to elucidate the role of loss-of-function *KCNH2* in epilepsy.

In this study, all deaths in the single mutant epilepsy and double mutant mice occurred following severe Racine 4-5 seizures resulting in tonic hind-limb extension. This sequence of events leading to death is commonly observed in mouse models of epilepsy and frequently used as a marker of SUDEP.[32, 49] However, as loss-of-function *Kcnh2* has been associated with convulsive syncope,[24, 30] it is essential to rule out these as contributing factors through concurrent ECoG and ECG recordings during terminal seizures. This can be technically challenging due to the rarity and unpredictability of such events, compounded by significant electromyographic noise during tonic hind-limb extension that compromises signal clarity. Additionally, post-mortem cardiac analysis was restricted by the sporadic nature of spontaneous deaths, making it nearly impossible to retrieve fresh tissue samples immediately. As such, while unlikely, we cannot completely rule out cardiogenic seizure or convulsive syncope as the underlying cause of sudden death in our mouse models.

Our *Kcnh2* mouse models robustly recorded prolonged QTc intervals. While this observation aligns with previous findings,[33, 35] other studies that utilised LQTS2 mouse models have reported conflicting phenotypes. Some have reported no ECG abnormalities despite complete loss of I_{Kr}, while others are embryonically lethal due to severe cardiac defects.[48] This highlights the need for further investigation into the developmental and electrophysiological contributions of *Kcnh2* in heart tissue.

Our study is not without limitations. The physiology of a mouse heart is significantly different to that of humans. Recapitulating our findings in larger animal models and in the clinical setting will be important next steps. Furthermore, we have not specifically monitored respiratory changes in our SUDEP mice. Although the cardiac-selective β-blocker is sufficient to protect against premature death, it is still possible that respiratory suppression could be part of the pathogenic cascade. More preclinical studies are also needed to investigate the interaction between seizures and other inherited arrhythmia syndromes. It is also important to note that atenolol's efficacy has yet to be tested in the single mutant *Gabrg2*$^{R43Q/+}$ mice due to the lower mortality rate. Although atenolol improves survival in the *Hcn1*$^{M294L/+}$ mice, the protective effect could be mediated through its impact on QT interval. As such, additional studies will need to be conducted in other genetic models of epilepsy to assess the protective effect of atenolol beyond QT prolongation.

Conclusion

In summary, we have provided evidence that *KCNH2*-caused LQTS contributes to higher SUDEP risk in two genetic epilepsy mouse models, and that β-blockers could be an effective treatment to improve survival. The genetic SUDEP mouse models will be useful preclinical tools to further dissect underlying mechanisms and test other cardiac-targeted therapies to reduce sudden death occurrence. While a 'unified' pathological mechanism underlying SUDEP

is unlikely, our data support the hypothesis that a cardiac-based mechanism can be part of the underlying pathological cascade leading to SUDEP.

Author contributions

CAR and MSS conceptualised and designed the study. MSS, AH, AK, ESMS, HML, CEM and AMP performed experiments. MSS, AH, AK, ESMS, HML and CAR performed data analyses. CAR, IES, SFB and MSS acquired funding for the project. MSS and CAR wrote the manuscript. MSS, ESMS, CEM, AMP, LEB, IES, CS, SFB and CAR revised the manuscript. All authors approved the final manuscript.

Acknowledgements

We thank Professor B. London of the University of Iowa for the *Kcnh2*$^{+/-}$ mice and their genetic information; Professor S. Petrou, Associate Professor S. Maljevic, Dr M. Li, Dr T. Karle and Professor I. Forster for technical advice and help with equipment and facility; Dr N. Jancovski for assistance with ECG technique; Professor A. Allen and Dr M. D. R. De Melo for advice with heart rate variability analysis; and Dr T. Lancefield for her assistance with identifying arrhythmias.

Funding information

This work was supported by an anonymous philanthropic gift for SUDEP research (to S.F.B. and I.E.S.). We would also like to acknowledge the CURE foundation, Medical Research Future Fund (#2016012) and National Health and Medical Research Council (#2019804) for support. C.S. and I.E.S. are recipients of National Health and Medical Research Council Practitioner Fellowships (#1154992 to C.S. and #1104831 to I.E.S.) and a Senior Investigator Fellowship (#2016822 to C.S. and #1172897 to I.E.S.). This work was also made possible through the Victorian State Government Operational Infrastructure Support and Australian Government National Health and Medical Research Council Independent Research Institute Infrastructure Support Scheme.

Conflict of interest statement

SFB declares unrestricted educational grants from UCB Pharma, SciGen and Eisai and consultancy fees from Praxis Precision Medicines. IES has served on scientific advisory boards for BioMarin, Chiesi, Eisai, Encoded Therapeutics, GlaxoSmithKline, Knopp Biosciences, Nutricia, Rogcon, Takeda Pharmaceuticals, UCB, Xenon Pharmaceuticals, Cerecin; has received speaker honoraria from GlaxoSmithKline, UCB, BioMarin, Biocodex, Chiesi, Liva Nova, Nutricia, Zuellig Pharma, Stoke Therapeutics and Eisai; has received funding for travel from UCB, Biocodex, GlaxoSmithKline, Biomarin, Encoded Therapeutics, Stoke Therapeutics and Eisai; has served as an investigator for Anavex Life Sciences, Cerevel Therapeutics, Eisai, Encoded Therapeutics, EpiMinder Inc, Epygenyx, ES-Therapeutics, GW Pharma, Marinus, Neurocrine BioSciences, Ovid Therapeutics, Takeda Pharmaceuticals, UCB, Ultragenyx, Xenon Pharmaceuticals, Zogenix and Zynerba; and has consulted for Care Beyond Diagnosis, Epilepsy Consortium, Atheneum Partners, Ovid Therapeutics, UCB, Zynerba Pharmaceuticals, BioMarin, Encoded Therapeutics and Biohaven Pharmaceuticals; and is a Non-Executive Director of Bellberry Ltd and a Director of the Australian Academy of Health and Medical Sciences and the Australian Council of Learned Academies Limited. She may accrue future revenue on pending patent WO61/010176 (filed: 2008): Therapeutic Compound; has a patent for SCN1A testing held by Bionomics Inc and licensed to various diagnostic companies; has a patent molecular diagnostic/theranostic target for benign familial infantile epilepsy (BFIE) [PRRT2] 2011904493 & 2012900190 and PCT/AU2012/001321 (TECH ID:2012-009). The remaining authors have no competing interests.

Data availability

Data may be shared upon reasonable request from the corresponding author.

Ethical publication statement

We confirm that we have read the Journal's position on issues involved in ethical publication and affirm that this report is consistent with those guidelines.

ORCID ID

Ming S. Soh (0000-0002-5689-2082)

Alibek Kuanyshbek (0000-0002-4886-2115)

Lauren E. Bleakley (0000-0001-5611-6860)

Christopher Semsarian (0000-0001-6441-274X)

Ingrid E. Scheffer (0000-0002-2311-2174)

Samuel F. Berkovic (0000-0003-4580-841X)

Christopher A. Reid (0000-0002-1457-8028)

References

1. World Health Organization. Epilepsy [online]. Available at: https://www.who.int/news-room/fact-sheets/detail/epilepsy. Accessed 17 May.

2. Devinsky O, Bundock E, Hesdorffer D, et al. Resolving ambiguities in SUDEP classification. *Epilepsia* 2018;**59**:1220-1233.

3. Nashef L, So EL, Ryvlin P, Tomson T. Unifying the definitions of sudden unexpected death in epilepsy. *Epilepsia* 2012;**53**:227-233.

4. Sveinsson O, Andersson T, Mattsson P, Carlsson S, Tomson T. Clinical risk factors in SUDEP: A nationwide population-based case-control study. *Neurology* 2020;**94**:e419-e429.

5. DeGiorgio CM, Markovic D, Mazumder R, Moseley BD. Ranking the leading risk factors for sudden unexpected death in epilepsy. *Front Neurol* 2017;**8**:1-6.

6. Opeskin K, Berkovic SF. Risk factors for sudden unexpected death in epilepsy: a controlled prospective study based on coroners cases. *Seizure* 2003;**12**:456-464.

7. Bagnall RD, Crompton DE, Semsarian C. Genetic basis of sudden unexpected death in epilepsy. *Front Neurol* 2017;**8**:348-348.

8. Devinsky O, Hesdorffer DC, Thurman DJ, Lhatoo S, Richerson G. Sudden unexpected death in epilepsy: epidemiology, mechanisms, and prevention. *Lancet Neurol* 2016;**15**:1075-1088.

9. Ryvlin P, Nashef L, Lhatoo SD, et al. Incidence and mechanisms of cardiorespiratory arrests in epilepsy monitoring units (MORTEMUS): a retrospective study. *Lancet Neurol* 2013;**12**:966-977.

10. Faingold CL, Feng HJ. A unified hypothesis of SUDEP: Seizure- induced respiratory depression induced by adenosine may lead to SUDEP but can be prevented by autoresuscitation and other restorative respiratory response mechanisms mediated by the action of serotonin on the periaqueductal gray. *Epilepsia* 2023;**64**:779–796.

11. Singh V, Ryan JM, Auerbach DS. It is premature for a unified hypothesis of sudden unexpected death in epilepsy: A great amount of research is still needed to understand the multisystem cascade. *Epilepsia* 2023;**00**:1-5.

12. Massey CA, Sowers LP, Dlouhy BJ, Richerson GB. Mechanisms of sudden unexpected death in epilepsy: the pathway to prevention. *Nat Rev Neurol* 2014;**10**:271-282.

13. Tester DJ, Ackerman MJ. Genetics of long QT syndrome. *Methodist Debakey Cardiovasc J* 2014;**10**:29-33.

14. Nei M. Cardiac effects of seizures. *Epilepsy Curr* 2009;**9**:91-95.

15. van der Lende M, Surges R, Sander JW, Thijs RD. Cardiac arrhythmias during or after epileptic seizures. *J Neurol Neurosurg Psychiatry* 2016;**87**:69-74.

16. Serdyuk S, Davtyan K, Burd S, et al. Cardiac arrhythmias and sudden unexpected death in epilepsy: Results of long-term monitoring. *Heart Rhythm* 2021;**18**:221-228.

17. Chahal CAA, Gottwald JA, St Louis EK, et al. QT prolongation in patients with index evaluation for seizure or epilepsy is predictive of all-cause mortality. *Heart Rhythm* 2021;**S1547-5271**:02346-02348.

18. Sivathamboo S, Friedman D, Laze J, et al. Association of short-term heart rate variability and sudden unexpected death in epilepsy. *Neurology* 2021;**97**:e2357-e2367.

19. Myers KA, Bello-Espinosa LE, Symonds JD, et al. Heart rate variability in epilepsy: A potential biomarker of sudden unexpected death in epilepsy risk. *Epilepsia* 2018;**59**:1372-1380.

20. Bagnall RD, Crompton DE, Petrovski S, et al. Exome-based analysis of cardiac arrhythmia, respiratory control, and epilepsy genes in sudden unexpected death in epilepsy. *Ann Neurol* 2016;**79**:522-534.

21. Aurlien D, Leren TP, Taubøll E, Gjerstad L. New *SCN5A* mutation in a SUDEP victim with idiopathic epilepsy. *Seizure* 2009;**18**:158-160.

22. Tu E, Bagnall RD, Duflou J, Semsarian C. Post-mortem review and genetic analysis of sudden unexpected death in epilepsy (SUDEP) cases. *Brain Pathol* 2011;**21**:201-208.

23. Smith JL, Anderson CL, Burgess DE, Elayi CS, January CT, Delisle BP. Molecular pathogenesis of long QT syndrome type 2. *J Arrhythm* 2016;**32**:373-380.

24. Sanchez-Conde FG, Jimenez-Vazquez EN, Auerbach DS, Jones DK. The ERG1 K+ channel and Its role in neuronal health and disease. *Front Mol Neurosci* 2022;**15**:890368.

25. Kang H, Lan L, Jia Y, et al. Long QT syndrome with potassium voltage-gated channel subfamily H member 2 gene mutation mimicking refractory epilepsy: case report. *BMC Neurol* 2021;**21**:338.

26. Shin SY, Hong JY, Lee DH. Delayed diagnosis of long QT syndrome in a patient with seizures. *Hong Kong J Emerg Med* 2019;**26**:190-193.

27. Anderson JH, Bos JM, Cascino GD, Ackerman MJ. Prevalence and spectrum of electroencephalogram-identified epileptiform activity among patients with long QT syndrome. *Heart Rhythm* 2014;**11**:53-57.

28. Auerbach DS, McNitt S, Gross RA, Zareba W, Dirksen RT, Moss AJ. Genetic biomarkers for the risk of seizures in long QT syndrome. *Neurology* 2016;**87**:1660-1668.

29. Johnson J, Hofman N, Haglund C, Cascino G, Wilde A, Ackerman M. Identification of a possible pathogenic link between congenital long QT syndrome and epilepsy. *Neurology* 2009;**72**:224-231.

30. Pascual JF, Marchite PJ, Silva JR, Gándara NR. Arrhythmic syncope: from diagnosis to management. *World J Cardiol* 2023;**15**:119.

31. Soh MS, Bagnall RD, Bennett MF, et al. Loss-of-function variants in the cardiac $K_v11.1$ channel as a genetic biomarker for SUDEP. *Ann Clin Transl Neurol* 2021;**8**:1422-1432.

32. Bleakley LE, McKenzie CE, Soh MS, et al. Cation leak underlies neuronal excitability in an HCN1 developmental and epileptic encephalopathy. *Brain* 2021;**144**:2060-2073.

33. Salama G, Baker L, Wolk R, Barhanin J, London B. Arrhythmia phenotype in mouse models of human long QT. *J Interv Card Electrophysiol* 2009;**24**:77-87.

34. Tan HO, Reid CA, Single FN, et al. Reduced cortical inhibition in a mouse model of familial childhood absence epilepsy. *Proc Natl Acad Sci U S A* 2007;**104**:17536-17541.

35. London B, Pan X-H, Lewarchik C, Lee JS. QT interval prolongation and arrhythmias in heterozygous Merg1-targeted mice. *Circulation* 1998;**98**:1-56.

36. Mitchell GF, Jeron A, Koren G. Measurement of heart rate and Q-T interval in the conscious mouse. *Am J Physiol* 1998;**274**:H747-751.

37. Petrou S, Reid CA. The GABAAγ2(R43Q) mouse model of human genetic epilepsy. In: Noebels JL, Avoli M, Rogawski MA, Olsen RW, Delgado-Escueta AV, eds. Jasper's basic mechanisms of the epilepsies. 4th edition ed: Bethesda (MD): National Center for Biotechnology Information (US), 2012.

38. Al-Khatib SM, Stevenson WG, Ackerman MJ, et al. 2017 AHA/ACC/HRS guideline for management of patients with ventricular arrhythmias and the prevention of sudden cardiac death: A report of the American College of Cardiology/American Heart Association Task Force on Clinical Practice Guidelines and the Heart Rhythm Society. *J Am Coll Cardiol* 2018;**72**:e91-e220.

39. Gruetter CA. Atenolol. In: Enna SJ, Bylund DB, eds. xPharm: The Comprehensive Pharmacology Reference. New York: Elsevier, 2007: 1-6.

40. Alimento M, Palermo P, Italiano G, Antonioli L, Salvioni E, Agostoni P. Can β-blockers influence regular daily physical activity? *J Hypertens* 2022;**40**:1199-1203.

41. Racine RJ. Modification of seizure activity by electrical stimulation. *Electroencephalogr Clin Neurophysiol* 1972;**32**:281–294.

42. Devinsky O. Effects of seizures on autonomic and cardiovascular function. *Epilepsy Curr* 2004;**4**:43–46.

43. Verrier RL, Dickerson LW, Nearing BD. Behavioral states and sudden cardiac death *Pacing Clin Electrophysiol* 1992;**15**:1387-1393.

44. Grandi E, Ripplinger CM. Antiarrhythmic mechanisms of beta blocker therapy. *Pharmacol Res* 2019;**146**:104274.

45. Nicolazzo JA, Steuten JA, Charman SA, Taylor N, Davies PJ, Petrou S. Brain uptake of diazepam and phenytoin in a genetic animal model of absence epilepsy. *Clin Exp Pharmacol Physiol* 2010;**37**:647-649.

46. Soh MS, Bagnall R, Semsarian C, Scheffer I, Berkovic SF, Reid CA. Rare SUDEP *SCN5A* variants cause changes in channel function implicating cardiac arrhythmia as a cause of death *Epilepsia* 2022;**63**:e57-62.

47. Zhou Y, Hao N, Sander J, Lin X, Xiong W, Zhou D. KCNH2 variants in a family with epilepsy and long QT syndrome: A case report and literature review. *Epileptic Disord* 2023;**25**:492-499.

48. Singh V, Wagner KT, Williams LG, et al. Knock-in Kcnh2 rabbit model of long QT syndrome type-2, epilepsy, and sudden death. *J Transl Med* 2025;**23**:446.

49. Smith J, Richerson G, Kouchi H, et al. Are we there yet? A critical evaluation of sudden and unexpected death in epilepsy models. *Epilepsia* 2024;**65**:9-25.

Figure legends

Figure 1. Characterisation of baseline epileptiform activity in all four genotypes of *Gabrg2*$^{R43Q/+}$ and *Kcnh2*$^{+/-}$ mating. (A) Example ECoG traces from a wild-type and a *Kcnh2*$^{+/-}$ mouse showing normal brain electrical activity. **(B-G)** Respective grey-highlighted areas in sample ECoG traces on the left from *Gabrg2*$^{R43Q/+}$ and *Gabrg2*$^{R43Q/+}$/*Kcnh2*$^{+/-}$ mice, and graphs on the right with mean ± SEM comparing the four genotypes, showing **(B-C)** interictal spike occurrence per hour, **(D-E)** abnormal discharges of spike-wave complex (SWDs) per hour, and **(F-G)** total number of ictal activities throughout the 24-hour recording. Spikes are brief, high-amplitude biphasic events; SWDs are rhythmic 5–8 Hz bursts with moderate amplitude; Racine stage ⩾3 seizures feature polyspike bursts and SWDs with motor symptoms like rearing or jumping. ** $P < 0.01$, **** $P < 0.0001$ using Kruskal-Wallis test with Dunn's post-hoc, N=10-13 mice/group. See Table S1 for summary of comparisons.

Figure 2. Loss-of-function *Kcnh2* causes QT prolongation in mice. (A) Example ECG traces showing sinus rhythm from a single wild-type, *Kcnh2*$^{+/-}$, *Gabrg2*$^{R43Q/+}$ or *Gabrg2*$^{R43Q/+}$/*Kcnh2*$^{+/-}$ mouse. The right traces, showing PQRST waves, are zoomed in from the grey-highlighted boxes from the respective left traces. The green-highlighted boxes on the zoomed-in traces on the right emphasise the difference in QT intervals between the four genotypes. **(B-C)** Violin distribution plots with mean ± SEM comparing **(B)** corrected QT interval (QTc), and **(C)** RR interval. **** $P < 0.0001$ using mixed model ANOVA with Tukey's multiple comparison, N=5-6 mice/group. All ECG parameters are summarised in Table S1.

Figure 3. Loss of *Kcnh2* function increases risk of premature mortality in *Gabrg2*$^{R43Q/+}$/*Kcnh2*$^{+/-}$ SUDEP mouse model, which is rescued by atenolol. (A) Kaplan-Meier survival curve demonstrating a lower survival rate in the *Kcnh2*$^{+/-}$, *Gabrg2*$^{R43Q/+}$ and

Gabrg2$^{R43Q/+}$/*Kcnh2*$^{+/-}$ mice. Video recordings confirmed that the *Gabrg2*$^{R43Q/+}$ and *Gabrg2*$^{R43Q/+}$/*Kcnh2*$^{+/-}$ mice died during Racine 4-5 seizure. **(B)** Kaplan-Meier survival curve demonstrating an improvement in survival of the double mutant mice that were given 0.6 g/L atenolol, but not in mice that were given 0.1 g/L atenolol. Atenolol was introduced at P40, marked by the **purple** arrow and line. * $P < 0.05$, **** $P < 0.0001$ compared to wild-type (in A) or untreated (in B) using Mantel-Cox log-rank test; N=9-45 mice/group.

Figure 4. Characterisation of baseline ECoG and ECG activity in all four genotypes of *Hcn1*$^{M294L/+}$ and *Kcnh2*$^{+/-}$ mating. (A-C) Graphs of mean ± SEM comparing baseline epileptiform activity throughout the 24-hour recording, including **(A)** interictal spikes, **(B)** spike-wave discharges (SWDs), and **(C)** spontaneous seizures, along with respective ECoG traces on top of the graphs. Spikes are brief, high-amplitude biphasic events; SWDs are rhythmic 5–8 Hz bursts with moderate amplitude; Racine stage ⩾3 seizures feature polyspike bursts and SWDs with motor symptoms like rearing or jumping. ** $P < 0.01$, *** $P < 0.001$, using Kruskal-Wallis test with Dunn's post-hoc, N=8-12 mice/group. **(D)** On the left are example ECG traces from a wild-type and *Hcn1*$^{M294L/+}$/*Kcnh2*$^{+/-}$ mouse. ECG traces on the right are zoomed-in from the **grey**-highlighted areas from respective ECG traces on the left, showing a higher heart rate and prolonged QT interval in the double mutant mice. **(E-F)** Violin plots with mean ± SEM comparing **(E)** QTc, and **(F)** RR interval between the four genotypes. *** $P < 0.001$ using mixed model ANOVA with Tukey's multiple comparison, N=6-12 mice/group. See Table S3 for summary of comparisons.

Figure 5. Increased risk of mortality in *Hcn1*$^{M294L/+}$/*Kcnh2*$^{+/-}$ SUDEP mouse model, which was rescued by cardiac-selective β-blocker atenolol. (A) Kaplan-Meier survival curve demonstrating that *Hcn1*$^{M294L/+}$ mice experienced a higher mortality rate. However, survival is even more reduced in the double mutant *Hcn1*$^{M294L/+}$/*Kcnh2*$^{+/-}$ mice. Video recordings

confirmed that the mice died during Racine 4-5 seizures. *N*=24-31 mice/group. **(B-C)** Like the *Gabrg2*$^{R43Q/+}$/*Kcnh2*$^{+/-}$ model, the cardiac-selective β-blocker atenolol (0.6 g/L) was able to reduce mortality in the **(B)** *Hcn1*$^{M294L/+}$/*Kcnh2*$^{+/-}$ and **(C)** *Hcn1*$^{M294L/+}$ mice. Atenolol was introduced at P21 (weaning age), marked by the **dark cyan** arrow and line. *N*=10-35 mice/group. * $P < 0.05$, **** $P < 0.0001$ compared to wild-type or untreated using Mantel-Cox log-rank test.

Figure 6. Effects of atenolol on ECG parameters during spontaneous seizures in *Hcn1*$^{M294L/+}$/*Kcnh2*$^{+/-}$ mice. (A) Representative ECG traces at baseline and during spontaneous seizures in untreated (top) and atenolol-treated (bottom) mice. QT intervals are highlighted in **green**. **(B-C)** Violin plots showing **(B)** QTc and **(C)** RR interval during baseline and seizures in untreated and atenolol-treated mice. *N*=3-6 mice/group. *** $P < 0.001$ using mixed model ANOVA with Tukey's multiple comparison (See Table S4 for summary of comparisons).

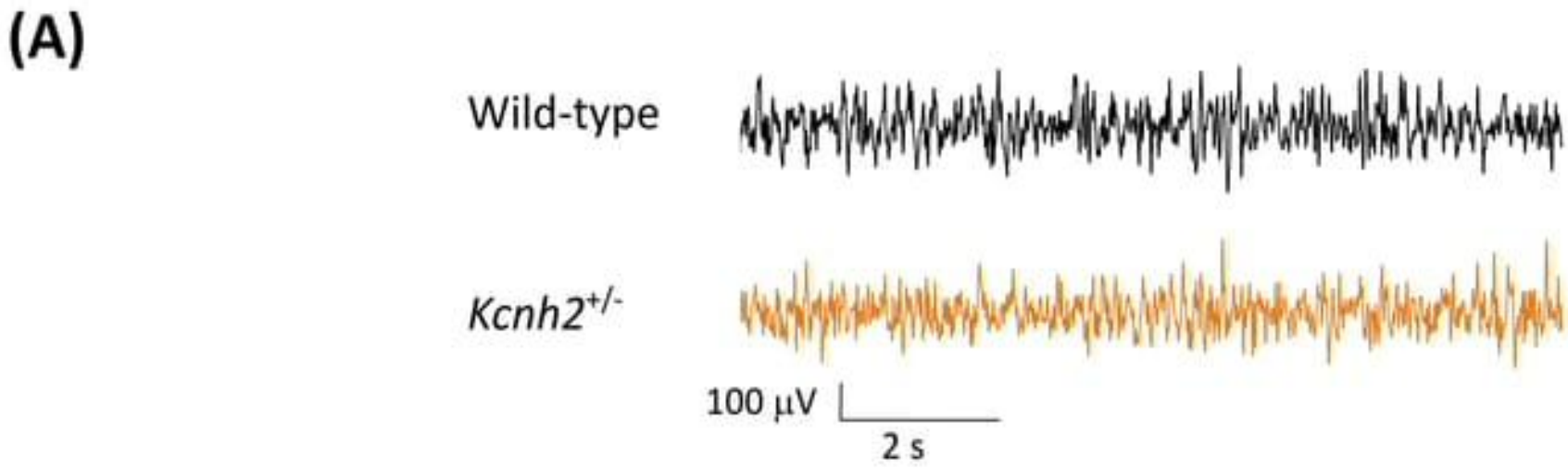
(A)
Wild-type
Kcnh2+/-
100 µV
2 s

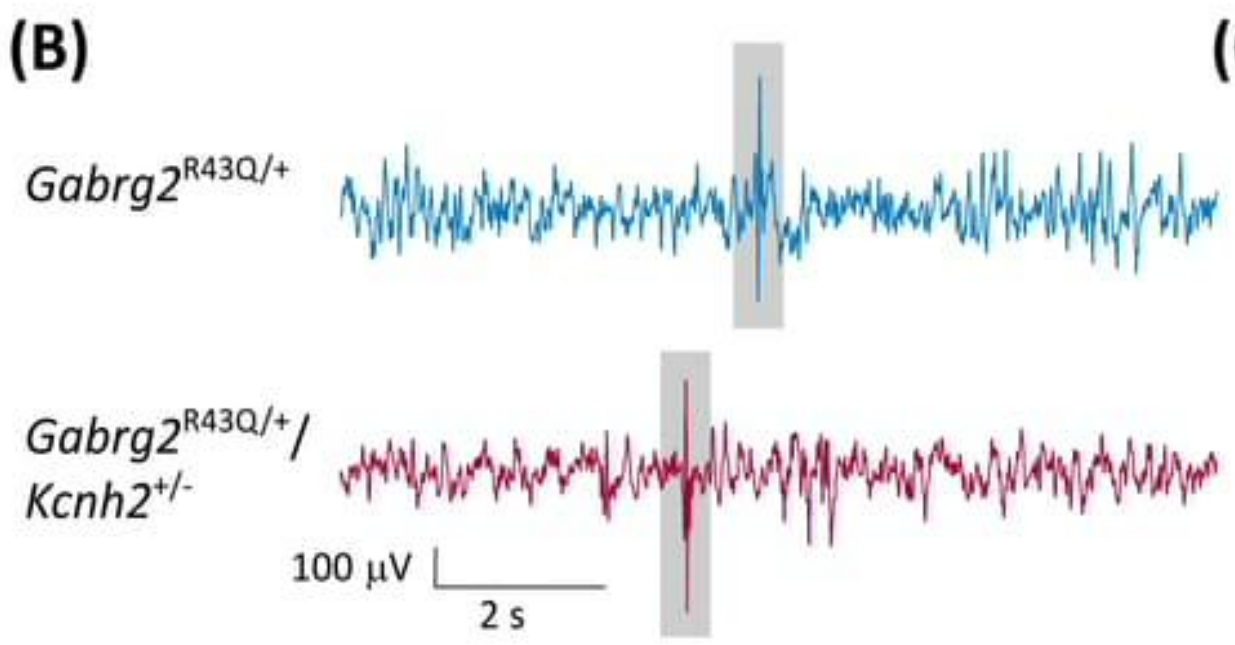
(B)
Gabrg2R43Q/+
Gabrg2R43Q/+/
Kcnh2+/-
100 µV
2 s

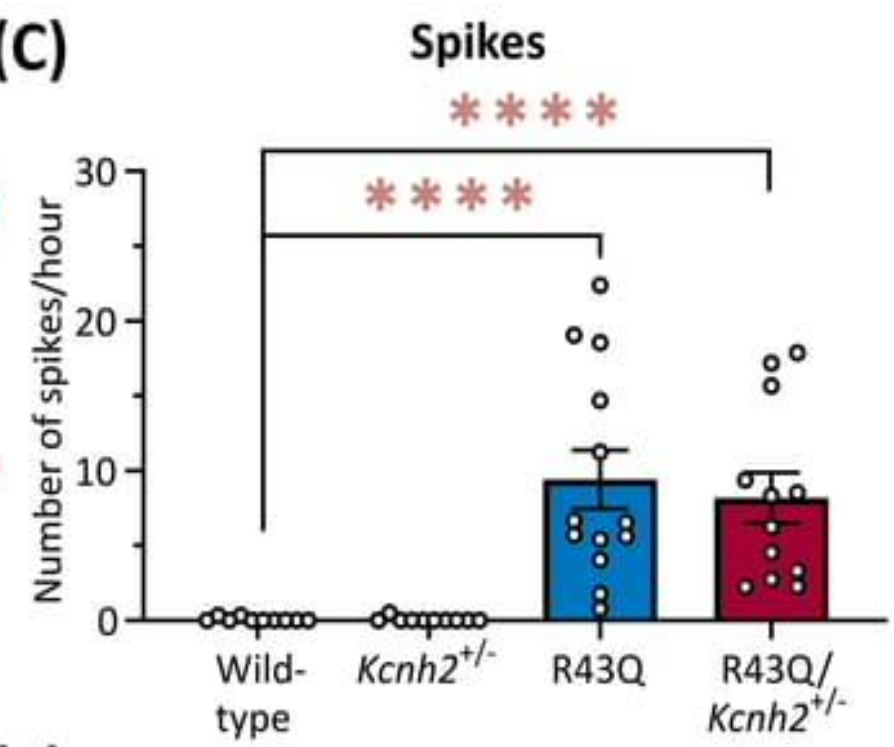
(C)
Spikes
Number of spikes/hour
Wild-type
Kcnh2+/-
R43Q
R43Q/Kcnh2+/-

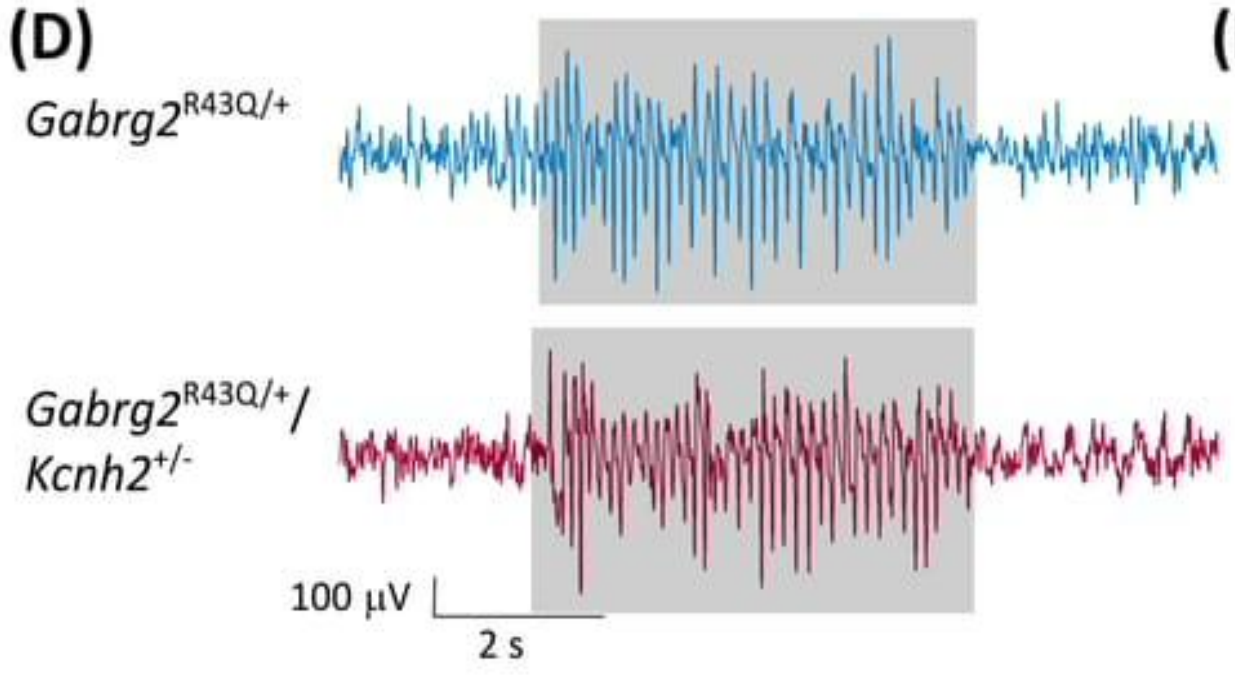
(D)
Gabrg2R43Q/+
Gabrg2R43Q/+/
Kcnh2+/-
100 µV
2 s

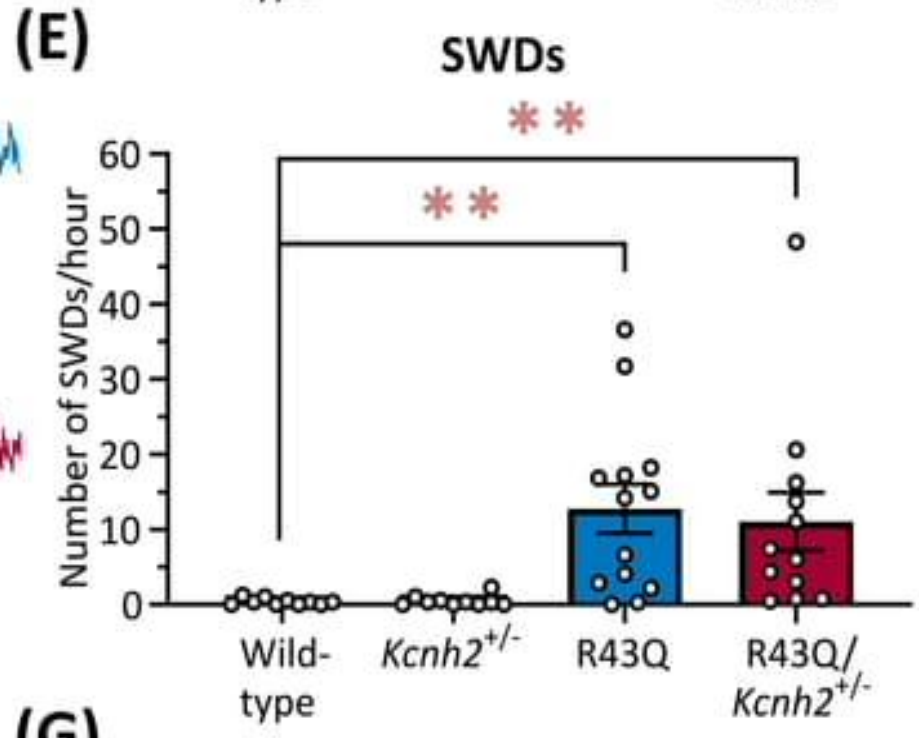
(E)
SWDs
Number of SWDs/hour
Wild-type
Kcnh2+/-
R43Q
R43Q/Kcnh2+/-

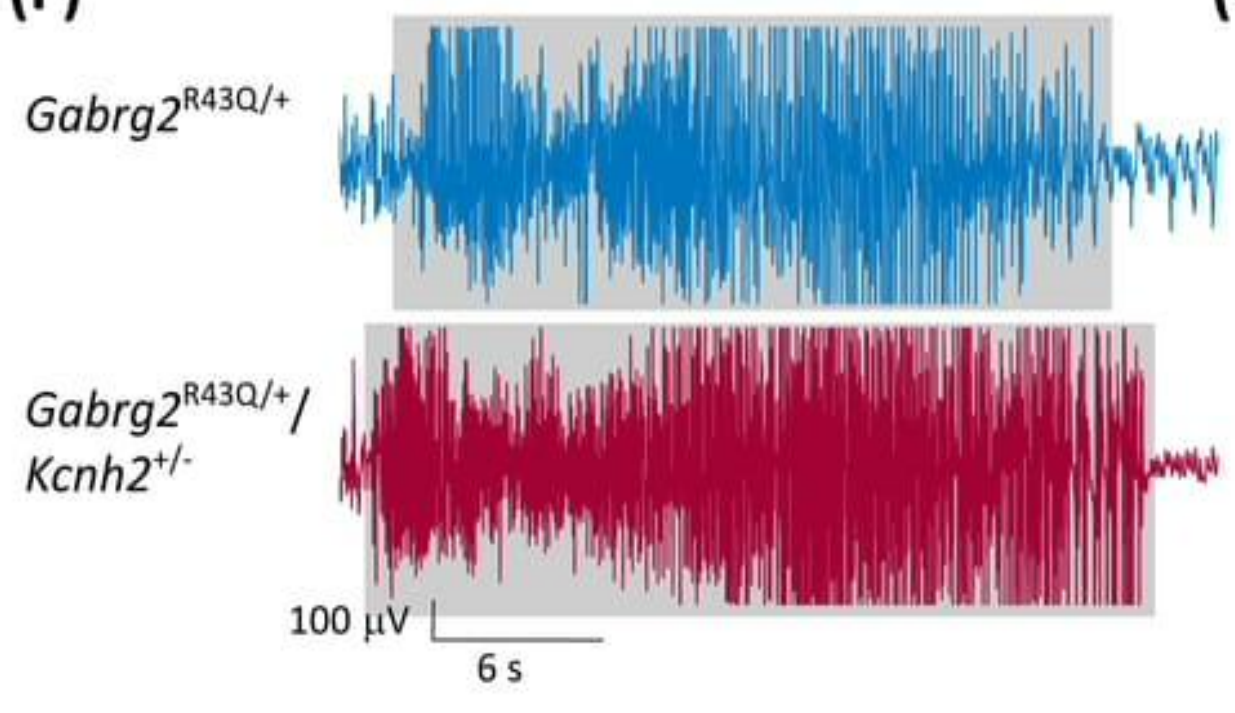
(F)
Gabrg2R43Q/+
Gabrg2R43Q/+/
Kcnh2+/-
100 µV
6 s

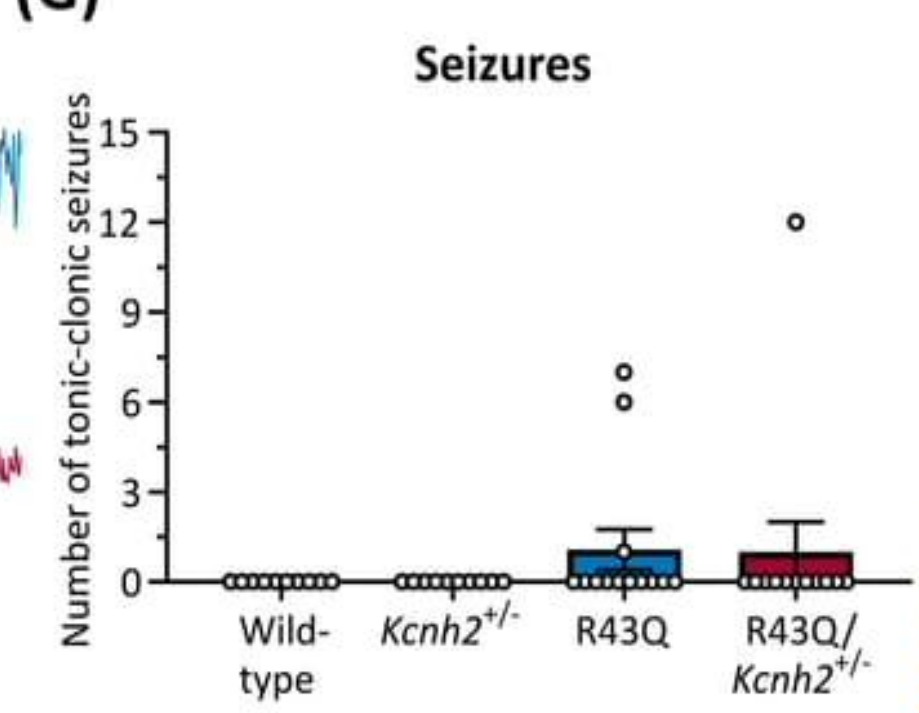
(G)
Seizures
Number of tonic-clonic seizures
Wild-type
Kcnh2+/-
R43Q
R43Q/Kcnh2+/-

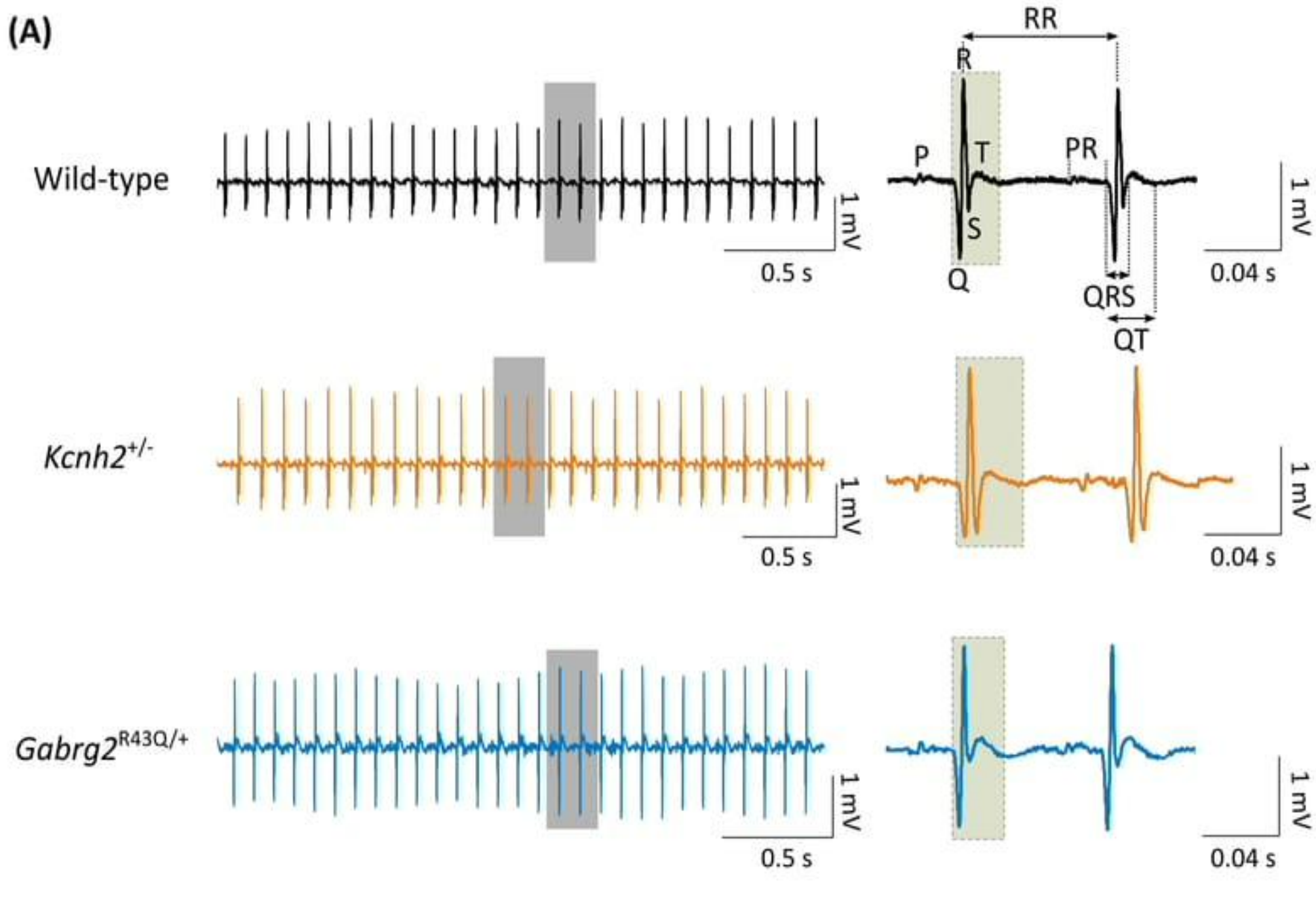
(A)
Wild-type
Kcnh2+/-
Gabrg2R43Q/+
Gabrg2R43Q/+ / Kcnh2+/-
RR
R
P
T
PR
S
Q
QRS
QT
1 mV
0.5 s
0.04 s

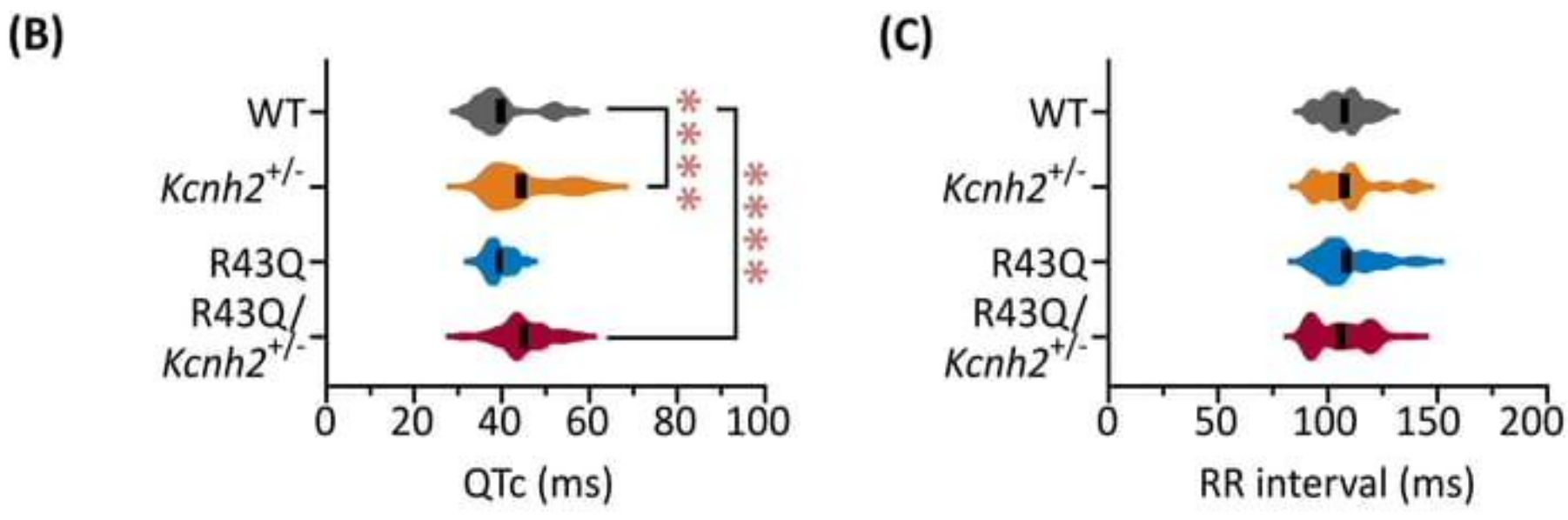
(B)
WT
Kcnh2+/-
R43Q
R43Q/ Kcnh2+/-
0 20 40 60 80 100
QTc (ms)
(C)
WT
Kcnh2+/-
R43Q
R43Q/ Kcnh2+/-
0 50 100 150 200
RR interval (ms)

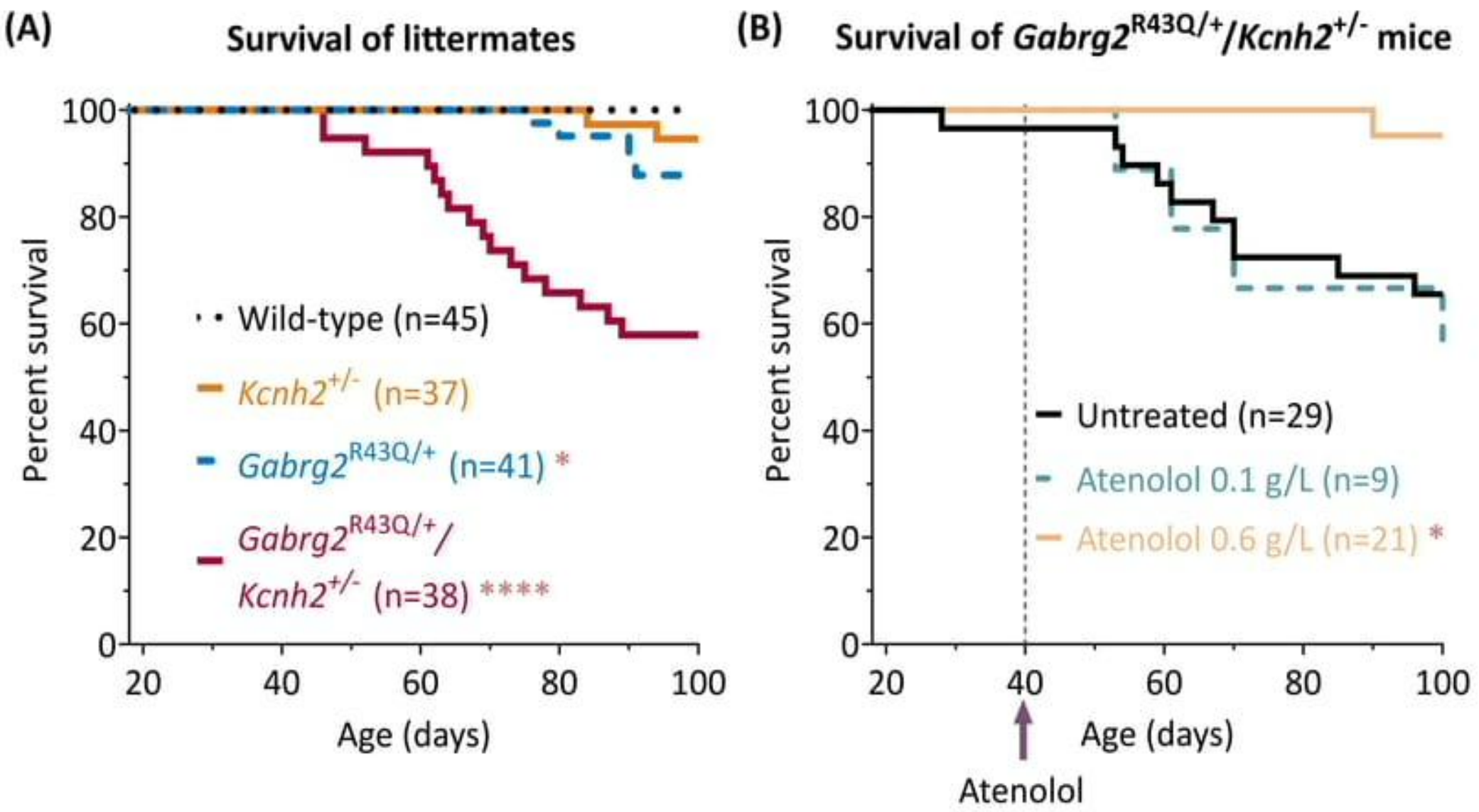
(A)
Survival of littermates
Percent survival
100
80
60
40
20
0
Wild-type (n=45)
Kcnh2+/- (n=37)
Gabrg2R43Q/+ (n=41) *
Gabrg2R43Q/+/
Kcnh2+/- (n=38) ****
20
40
60
80
100
Age (days)
(B)
Survival of Gabrg2R43Q/+/Kcnh2+/- mice
Percent survival
Untreated (n=29)
Atenolol 0.1 g/L (n=9)
Atenolol 0.6 g/L (n=21) *
Atenolol
Age (days)

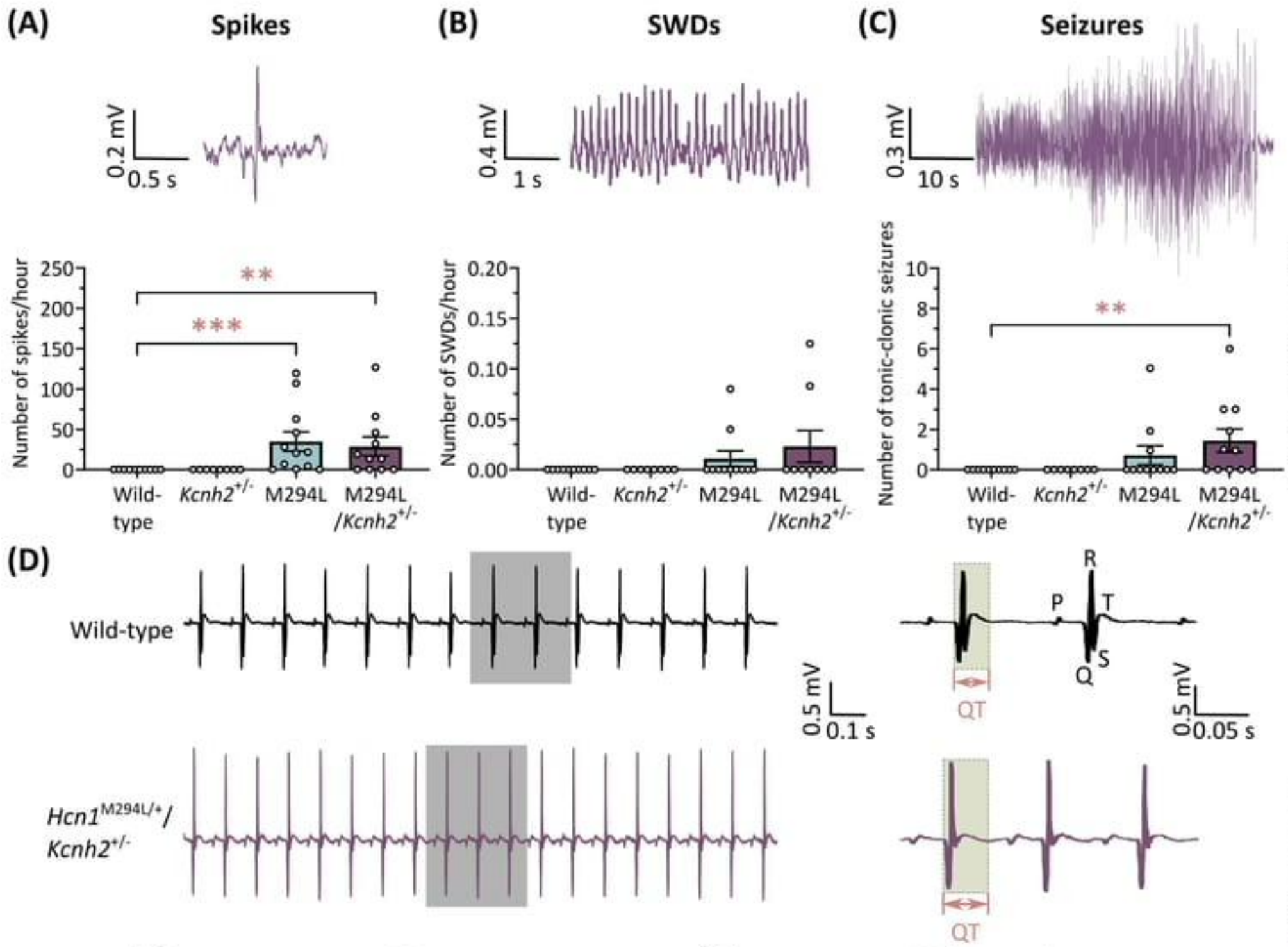
(A)
Spikes
0.2 mV
0.5 s
Number of spikes/hour
250
200
150
100
50
0
**
***
Wild-type
Kcnh2+/-
M294L
M294L /Kcnh2+/-
(B)
SWDs
0.4 mV
1 s
Number of SWDs/hour
0.20
0.15
0.10
0.05
0.00
Wild-type
Kcnh2+/-
M294L
M294L /Kcnh2+/-
(C)
Seizures
0.3 mV
10 s
Number of tonic-clonic seizures
10
8
6
4
2
0
**
Wild-type
Kcnh2+/-
M294L
M294L /Kcnh2+/-
(D)
Wild-type
Hcn1M294L/+/ Kcnh2+/-
0.5 mV
0.1 s
R
P
T
Q
S
QT
0.5 mV
0.05 s
QT
(E)
QTc
QTc (ms)
150
100
50
0
***
***
***
Wild-type
Kcnh2+/-
M294L
M294L /Kcnh2+/-
(F)
RR interval
RR interval (ms)
320
240
160
80
0
***
***
Wild-type
Kcnh2+/-
M294L
M294L /Kcnh2+/-

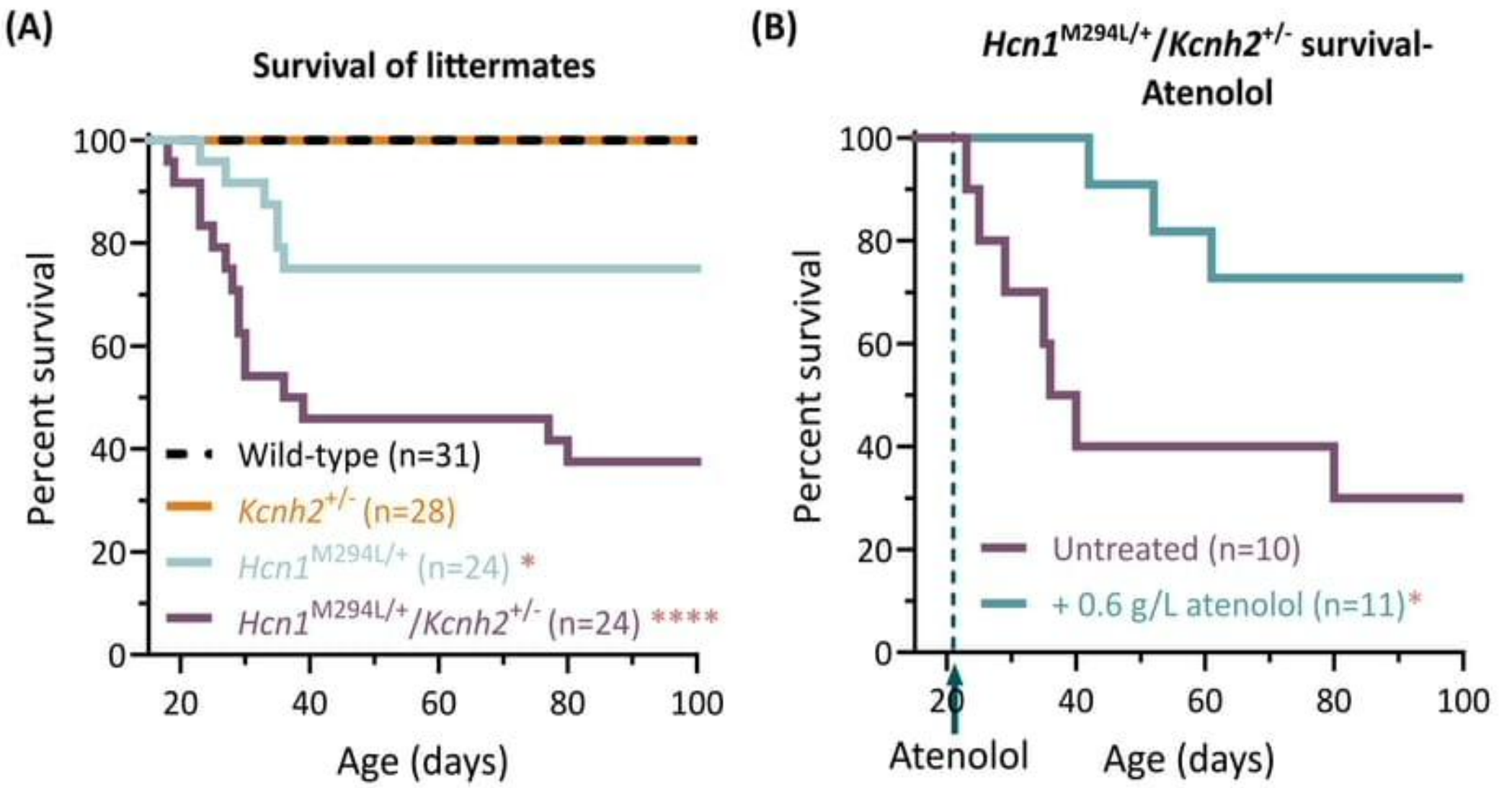
(A)
Survival of littermates
Percent survival
100
80
60
40
20
0
Wild-type (n=31)
Kcnh2+/- (n=28)
Hcn1M294L/+ (n=24) *
Hcn1M294L/+/Kcnh2+/- (n=24) ****
20
40
60
80
100
Age (days)
(B)
Hcn1M294L/+/Kcnh2+/- survival-Atenolol
Percent survival
Untreated (n=10)
+ 0.6 g/L atenolol (n=11)*
Atenolol
Age (days)

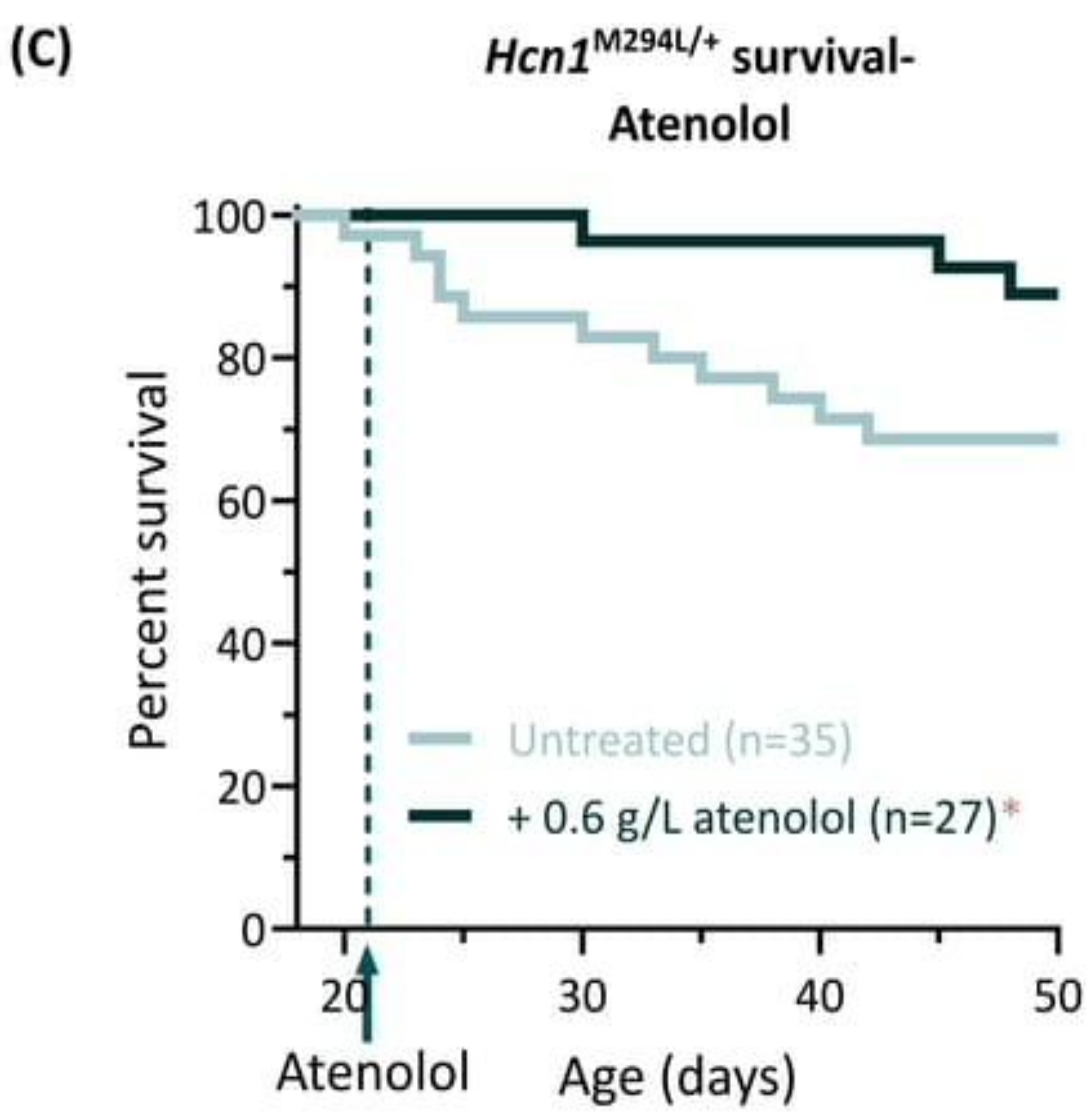
(C)
Hcn1M294L/+ survival-Atenolol
Percent survival
100
80
60
40
20
0
Untreated (n=35)
+ 0.6 g/L atenolol (n=27)*
20
30
40
50
Atenolol
Age (days)

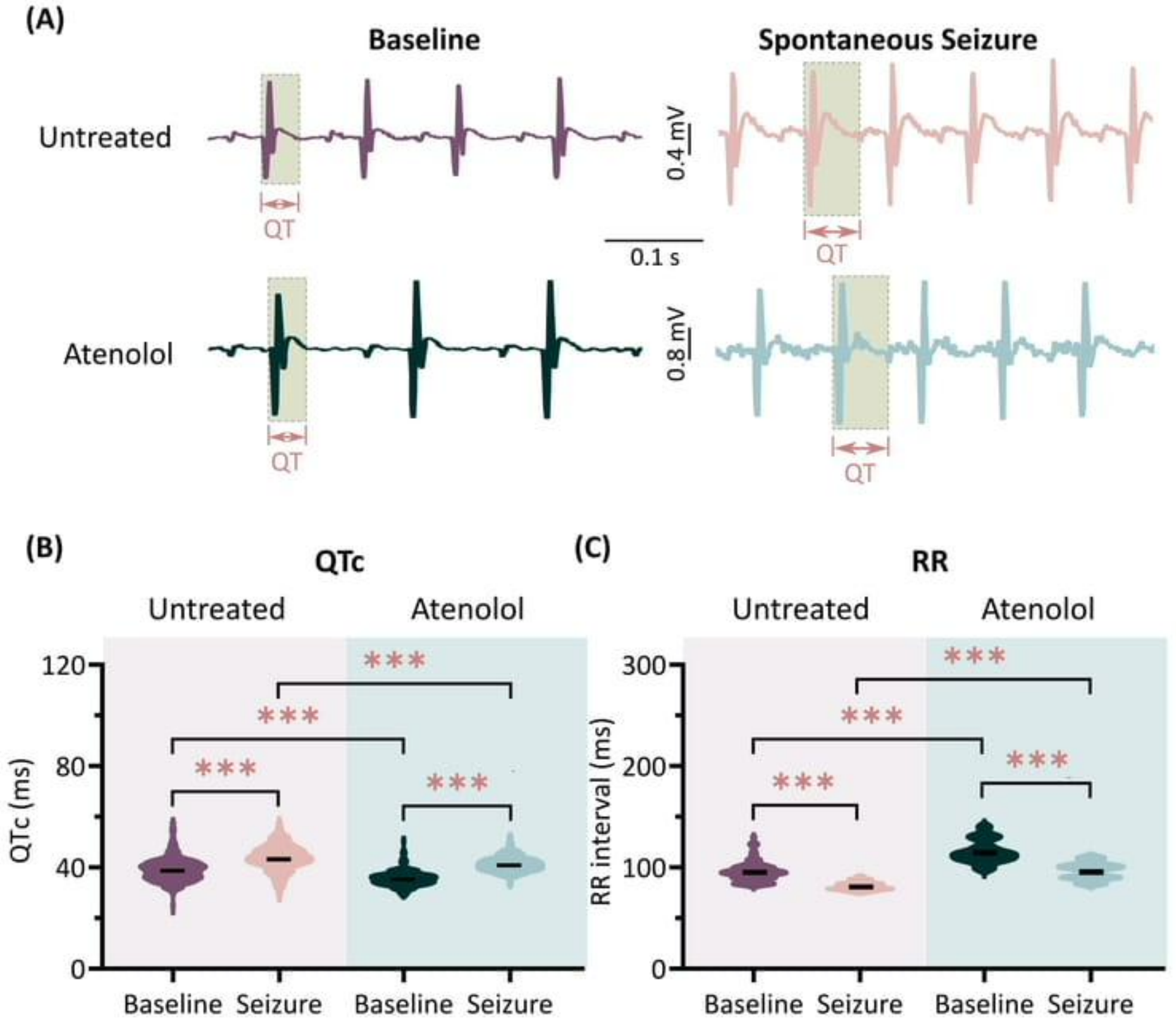
(A)
Baseline
Spontaneous Seizure
Untreated
Atenolol
0.4 mV
0.8 mV
0.1 s
QT
(B)
QTc
Untreated
Atenolol
QTc (ms)
120
80
40
0
***
Baseline
Seizure
(C)
RR
RR interval (ms)
300
200
100

Supplementary Materials and Methods (Appendix S1)

Atenolol rescues premature mortality in genetic mouse models of sudden unexpected death in epilepsy.

Ming S. Soh[1], Amanda Hu[1], Alibek Kuanyshbek[1], Erlina S. Mohamed Syazwan[1], Hian M. Lee[1], Chaseley E. McKenzie[1], A. Marie Phillips[1,2], Lauren E. Bleakley[1], Christopher Semsarian[3,4,5], Ingrid E. Scheffer[1,6,7,8], Samuel F. Berkovic[6], Christopher A. Reid[1]

Author affiliations:

[1]The Florey Institute of Neuroscience and Mental Health, University of Melbourne, Parkville, VIC, Australia

[2]School of Biosciences, University of Melbourne, Melbourne, VIC, Australia

[3]Agnes Ginges Centre for Molecular Cardiology at Centenary Institute, The University of Sydney, Sydney, NSW, Australia

[4]Faculty of Medicine and Health, The University of Sydney, NSW, Australia

[5]Department of Cardiology, Royal Prince Alfred Hospital, Sydney, NSW, Australia

[6]Epilepsy Research Centre, Department of Medicine, University of Melbourne, Austin Health, Heidelberg, VIC, Australia

[7]Murdoch Children's Research Institute, The Royal Children's Hospital, Parkville, VIC, Australia

[8]Department of Paediatrics, University of Melbourne, Royal Children's Hospital, VIC, Australia

Animal study approval

Experiments involving animals were performed in accordance with the Prevention of Cruelty to Animals Act, 1986 under the guidelines of the National Health and Medical Research Council (NHMRC) of Australia Code of Practice for the Care and Use of Animals for Experimental Purposes. All procedures and monitoring include standard operating protocols that were approved by the Animal Ethics Committee at the Florey Institute of Neuroscience and Mental Health. At the conclusion of experimentation, mice were culled by cervical dislocation or decapitation following deep isoflurane anaesthesia, which are Australian & New Zealand Council for the Care of Animals in Research and Teaching (ANZCCART) approved methods.

Animal housing and maintenance

Gabrg2$^{R43Q/+}$ and *Kcnh2*$^{+/-}$ strains were maintained on a DBA/2J background, *Hcn1*$^{M294L/+}$ was maintained on a C57BL/6J. All strains had been backcrossed for at least 10 generations. The mating between *Gabrg2*$^{R43Q/+}$ and *Kcnh2*$^{+/-}$, and *Hcn1*$^{M294L/+}$ and *Kcnh2*$^{+/-}$ mice was performed on-site at the Florey Institute of Neuroscience and Mental Health, yielding wild-type, *Gabrg2*$^{R43Q/+}$, *Kcnh2*$^{+/-}$, or *Gabrg2*$^{R43Q/+}$/*Kcnh2*$^{+/-}$ offspring for the *Gabrg2*$^{R43Q/+}$ and *Kcnh2*$^{+/-}$ cross, and wild-type, *Hcn1*$^{M294L/+}$, *Kcnh2*$^{+/-}$, or *Hcn1*$^{M294L/+}$/*Kcnh2*$^{+/-}$ offspring for the *Hcn1*$^{M294L/+}$ and *Kcnh2*$^{+/-}$ cross.

Mice were toe-clipped and genotyped at P7, weaned at P21-23, and group-housed once weaned until experiments. The housing was within standard 15 × 30 × 12 cm cages (Techniplast, Westchester, PA, USA) maintained under 12-h dark and light (<50 lux) cycles, in ambient temperature, quiet condition, and with access to dry pellet food and tap water *ad libitum*. For each experimental comparison, age-matched littermate controls were used. Mice aged P≥25 were used for experiments. Prior to experiments, mice were acclimatised to experimental rooms for at least an hour. Sample sizes were estimated using power analysis (G*Power) based

on observed effect size and a type one error rate of 0.05. Approximately equal numbers of male and female mice were used with common controls where appropriate. Blinding and randomisation of treatment and analyses (video, electrocorticography, electrocardiography) to genotypes were routine.

Survival recording and treatment study

Mice were checked daily and weighed weekly during the duration of recording, with free continuous access to food and water. Video analyses of seizures and deaths were completed off-line. Amount drunk was measured daily for both untreated and atenolol-treated mice. Drinking water for both groups was replaced with fresh solution every 3 days.

Implantation electrocorticography and electrocardiogram electrodes

4-5% and 1-1.5% isoflurane was used for anaesthesia induction and maintenance, respectively. Anaesthetised mice were secured on a stereotaxic frame with heating pad. Following administration of subcutaneous anaesthetic lignocaine (6 mg/kg) and analgesic meloxicam (3 mg/kg) at the incision site perioperatively, an incision was made on the scalp to expose the skull between lambda and bregma, where three holes, each approximately 1 mm in diameter, were drilled. Two of these were positioned bilaterally over the somatosensory cortex, with the third located caudal to the lambdoid suture 0.5 mm lateral from the midline towards the right side of the skull. Stainless steel 0.10” screws (Pinnacle Technology Inc., Lawrence, KS, USA) pre-soldered with silver wire electrodes (AD instruments, Colorado Springs, CO, USA) were implanted into each hole, with the anterior two screws implanted epidurally and used as the active channel electrodes, and the posterior screw implanted slightly more shallowly and used as the reference channel electrode. A ground electrode made of silver wire was affixed to the skull immediately caudal to the lambdoid suture 0.5 mm lateral from the midline towards the left side of the skull. The silver wires of the reference, ground, and two active channel

electrodes were soldered to a head mount (Pinnacle technology Inc., Lawrence, KS, USA), held in place by self-curing acrylic resin.

To place the ECG wires (Axon Connect Pte Ltd, Singapore) that had been pre-soldered to the head mount with the ECoG electrodes, an incision was made on the skin just below the head mount and on both lateral sides. Each ECG wire was tunnelled underneath the skin through the incisions, before it was sutured to the left or right muscle layer under the skin between the heart and vertebrochondral ribs with 5-0 silk suture. Incision wounds on the skin were sutured with absorbable 4-0 suture. Mice were allowed to recover for at least one week prior to experimentation.

Electrocorticography and electrocardiogram recording

All ECoG and ECG recordings were performed on conscious mice. Each mouse was placed into individual clear plexiglass containers (140 cm x 175cm x 140 cm) with standard bedding, food and water, during each ECoG and ECG recording. Head mount was connected to a preamplifier with 10x amplification (Pinnacle Technology Inc., Lawrence, KS, USA), which in turn was connected to a data acquisition system (Sirenia 2.1.0, Pinnacle technology Inc., Lawrence, KS, USA). ECoG and ECG data were sampled at 2 kHz[1] and 500 Hz low-pass filtered. Each set-up was also connected to an in-built dome camera (320 x 240, 20 fps, Pinnacle technology Inc., Lawrence, KS, USA) for synchronised video recording.

Baseline epileptiform analysis

The entire 24-hour ECoG recording was visually analysed for spikes, spike-wave discharges (SWDs) and seizures using Sirenia software (version 2.1.0, Pinnacle technology Inc., Lawrence, KS, USA). A spike was defined by biphasic events lasting <200 ms with approximately thrice

the amplitude of baseline ECoG activity.[2] An SWD was characterised by burst frequency typically between 5-8 Hz, 2-3x larger amplitude than baseline, with limited spike-to-spike variability.[3] A full Racine stage 3 and above seizure generally had a combination of large-amplitude polyspike bursts and spike-wave discharges accompanied by behavioural changes such as forelimb clonus, rearing or wild jumping.[4]

Analysis of cardiac parameters

30-50 consecutive beats from three to six sections throughout the ECG recording were manually analysed and values averaged. For baseline comparison, only segments with reliable sinus rhythm were used for analyses. ECG parameters that were analysed included P-wave, PR, RR QRS, and QT intervals. Measurement of QT interval was made at T-wave anti-peak according to published methodology, to account for the unique T-wave morphology in mice.[5]

Heart samples for heart weight to body weight ratio

Littermates aged P70-90 from the *Gabrg2*$^{R43Q/+}$ and *Kcnh2*$^{+/-}$ cross were weighed before they were euthanised via cervical dislocation following deep isoflurane anaesthesia. Their hearts were excised, washed in PBS and blotted dry on paper towel. The individual hearts were then weighed to obtain heart weight to body weight ratio.

References

1. Mishra V, Gautier NM, Glasscock E. Simultaneous video-EEG-ECG monitoring to identify neurocardiac dysfunction in mouse models of epilepsy. Journal of visualized experiments: JoVE 2018:57300.

2. Bleakley LE, McKenzie CE, Soh MS, et al. Cation leak underlies neuronal excitability in an HCN1 developmental and epileptic encephalopathy. Brain 2021;144:2060-2073.

3. Tan HO, Reid CA, Single FN, et al. Reduced cortical inhibition in a mouse model of familial childhood absence epilepsy. Proc Natl Acad Sci U S A 2007;104:17536-17541.

4. Racine RJ. Modification of seizure activity by electrical stimulation. Electroencephalogr Clin Neurophysiol 1972;32:281–294.

5. Ha TW, Oh B, Kang J-O. Electrocardiogram recordings in anesthetized mice using lead II. J Vis Exp 2020:e61583.

Supplementary Figures and Videos

Atenolol rescues premature mortality in genetic mouse models of sudden unexpected death in epilepsy.

Ming S. Soh[1], Amanda Hu[1], Alibek Kuanyshbek[1], Erlina S. Mohamed Syazwan[1], Hian M. Lee[1], Chaseley E. McKenzie[1], A. Marie Phillips[1,2], Lauren E. Bleakley[1], Christopher Semsarian[3,4,5], Ingrid E. Scheffer[1,6,7,8], Samuel F. Berkovic[6], Christopher A. Reid[1]

Author affiliations:

[1]The Florey Institute of Neuroscience and Mental Health, University of Melbourne, Parkville, VIC, Australia

[2]School of Biosciences, University of Melbourne, Melbourne, VIC, Australia

[3]Agnes Ginges Centre for Molecular Cardiology at Centenary Institute, The University of Sydney, Sydney, NSW, Australia

[4]Faculty of Medicine and Health, The University of Sydney, NSW, Australia

[5]Department of Cardiology, Royal Prince Alfred Hospital, Sydney, NSW, Australia

[6]Epilepsy Research Centre, Department of Medicine, University of Melbourne, Austin Health, Heidelberg, VIC, Australia

[7]Murdoch Children's Research Institute, The Royal Children's Hospital, Parkville, VIC, Australia

[8]Department of Paediatrics, University of Melbourne, Royal Children's Hospital, VIC, Australia

Supplementary Figures

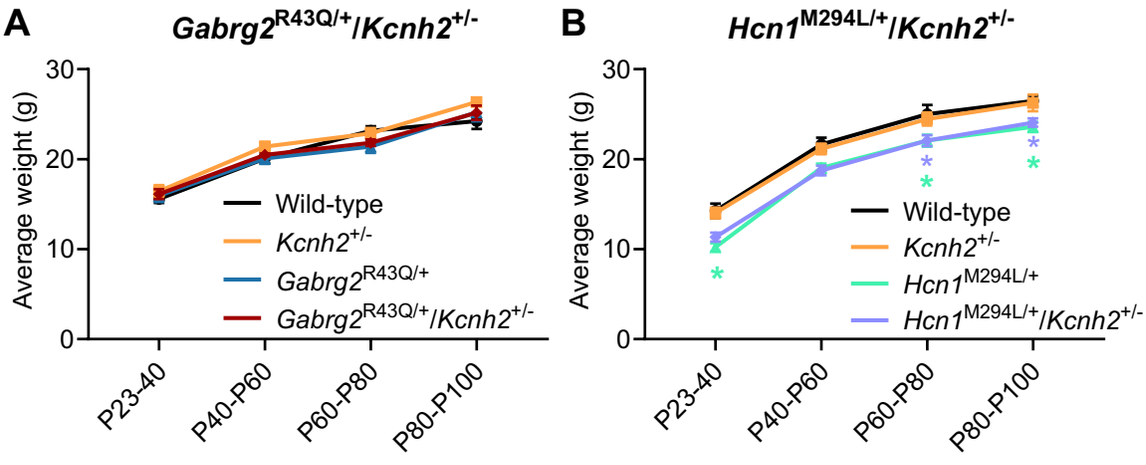

Figure S1: Average weight of littermates. (A) Littermates from *Gabrg2*$^{R43Q/+}$ and *Kcnh2*$^{+/-}$ cross had similar weights across the four genotypes. **(B)** On the other hand, *Hcn1*$^{M294L/+}$ and *Hcn1*$^{M294L/+}$/*Kcnh2*$^{+/-}$ littermates were smaller compared to their wild-type or *Kcnh2*$^{+/-}$ counterpart. Values were plotted as mean ± SEM; Mixed model ANOVA with Tukey's posthoc compared to wild-type values within each age group, N = 24-45/group, * $P < 0.05$. Full statistical comparison is listed in Table S1 and S3.

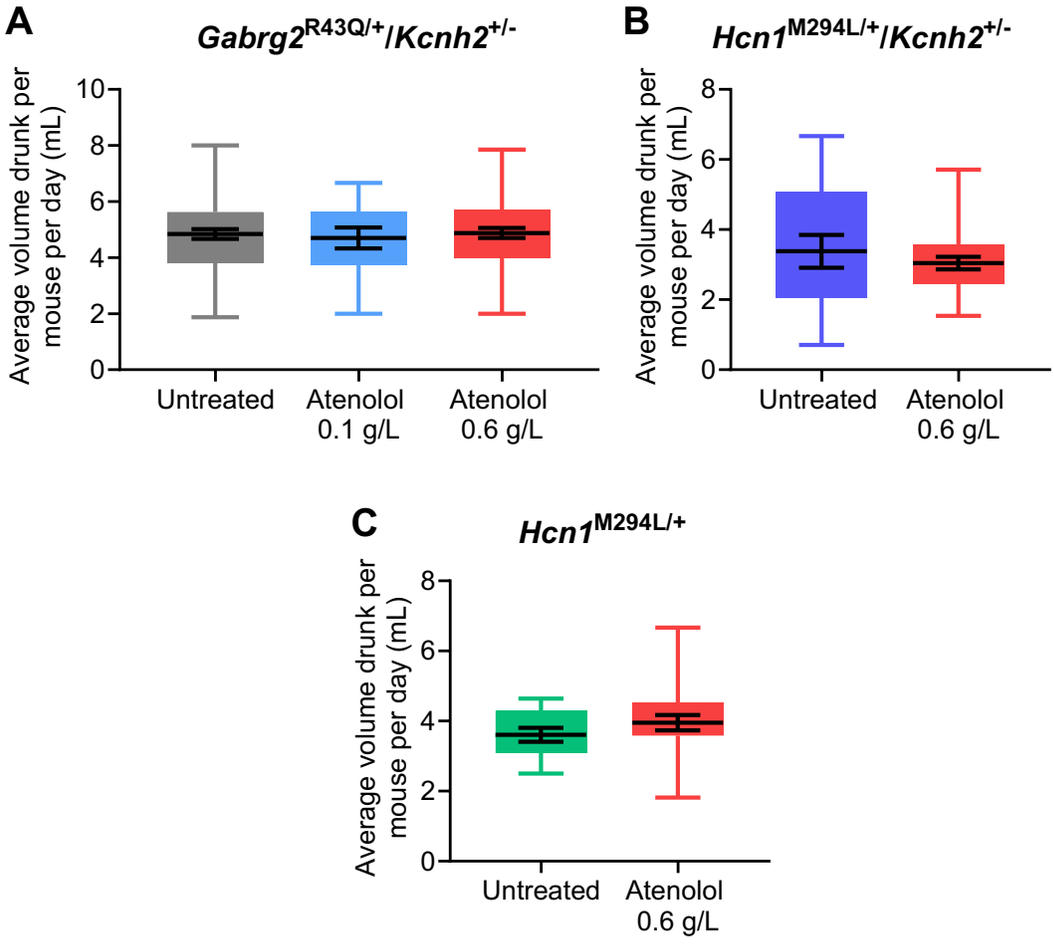

Figure S2: Average volume of water drunk per mouse per day. Comparison of volume drunk daily per **(A)** *Gabrg2*$^{R43Q/+}$/*Kcnh2*$^{+/-}$, **(B)** *Hcn1*$^{M294L/+}$/*Kcnh2*$^{+/-}$ or **(C)** *Hcn1*$^{M294L/+}$ mouse revealed no difference between the treatment groups. Graphs were plotted as box and whiskers with mean ± SEM. Kruskal-Wallis test with Dunn's posthoc, compared to untreated, was used for (A), while Student's *t*-test was used for (B) and (C); N = 9-29 animals per group, $P > 0.05$.

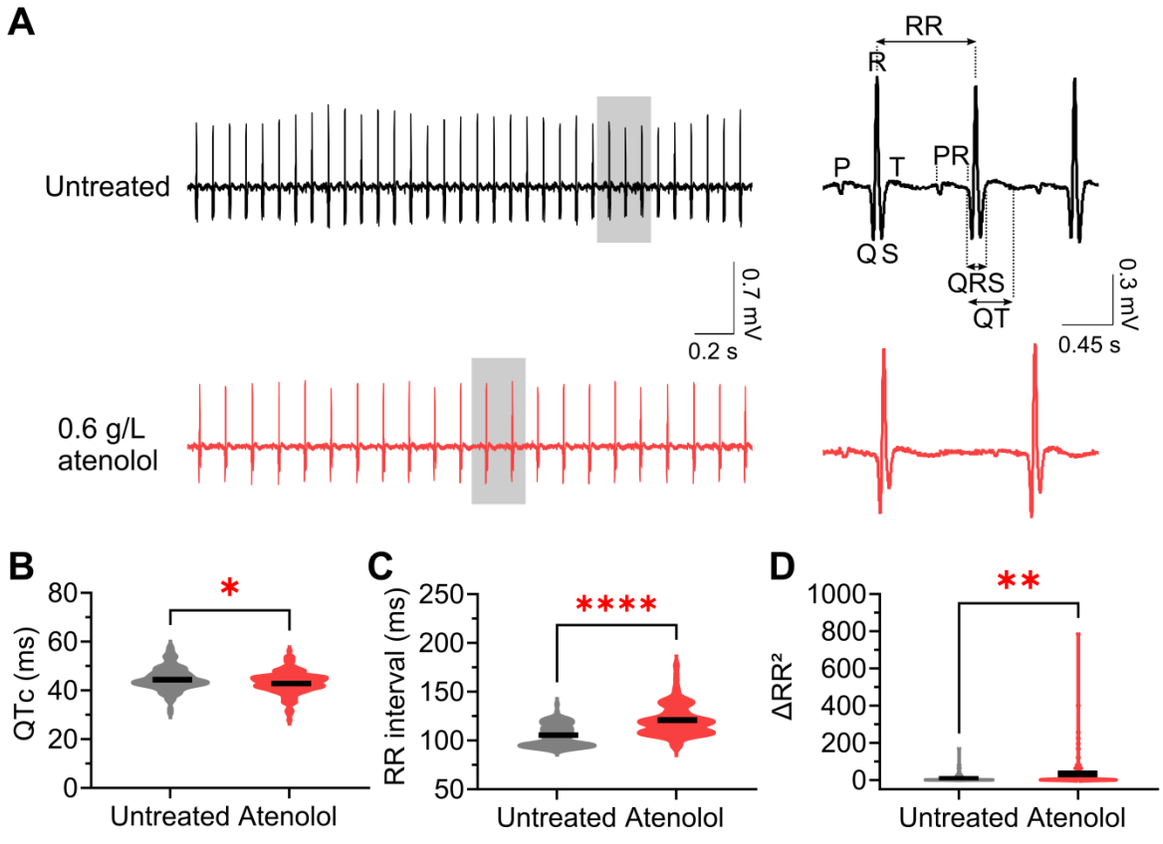

Figure S3. Atenolol significantly reduces heart rate and QTc in *Gabrg2*$^{R43Q/+}$/*Kcnh2*$^{+/-}$ mice. (A) Example ECG traces from a single untreated and 0.6 g/L atenolol-treated *Gabrg2*$^{R43Q/+}$/*Kcnh2*$^{+/-}$ mouse. The right traces are zoomed in from the grey-highlighted boxes from the respective left traces. **(B-D)** Violin distribution plots with mean ± SEM comparing **(B)** corrected QT interval (QTc), **(C)** RR interval, and **(D)** squared differences between successive RR intervals, a component of heart rate variability. Mixed model ANOVA with Tukey's multiple comparison * $P < 0.05$, ** $P < 0.01$, **** $P < 0.0001$, N=6-7 mice per group. Other ECG parameters are summarised in Table S2.

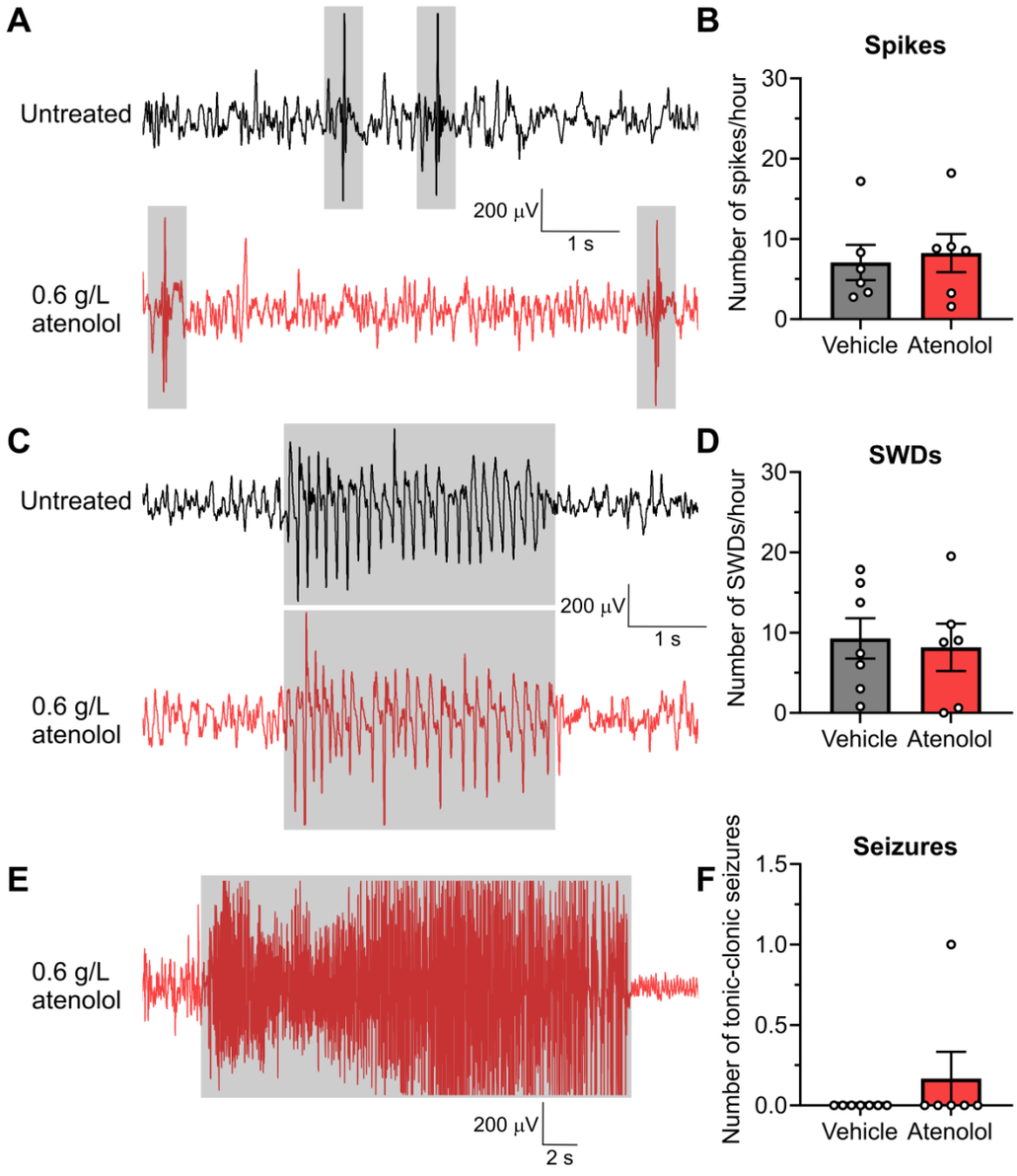

Figure S4: Atenolol does not affect seizure phenotype in *Gabrg2*$^{R43Q/+}$/*Kcnh2*$^{+/-}$ mice. **(A-F)** Respective grey-highlighted areas in sample ECoG traces on the left from untreated or 0.6 g/L atenolol-treated *Gabrg2*$^{R43Q/+}$/*Kcnh2*$^{+/-}$ mice, and graphs on the right with mean ± SEM comparing between the two groups, showing **(A-B)** number of spikes per hour, **(C-D)** spike-wave discharge events (SWDs) per hour, and **(E-F)** total number of seizures within a 24-hour period (see Table 2). $P > 0.05$ between the two groups for all three parameters. Student's *t*-test was used for **(B)** and **(D)**, while Mann-Whitney U-test was used for **(F)**, N=6-7 mice per group (Table S2).

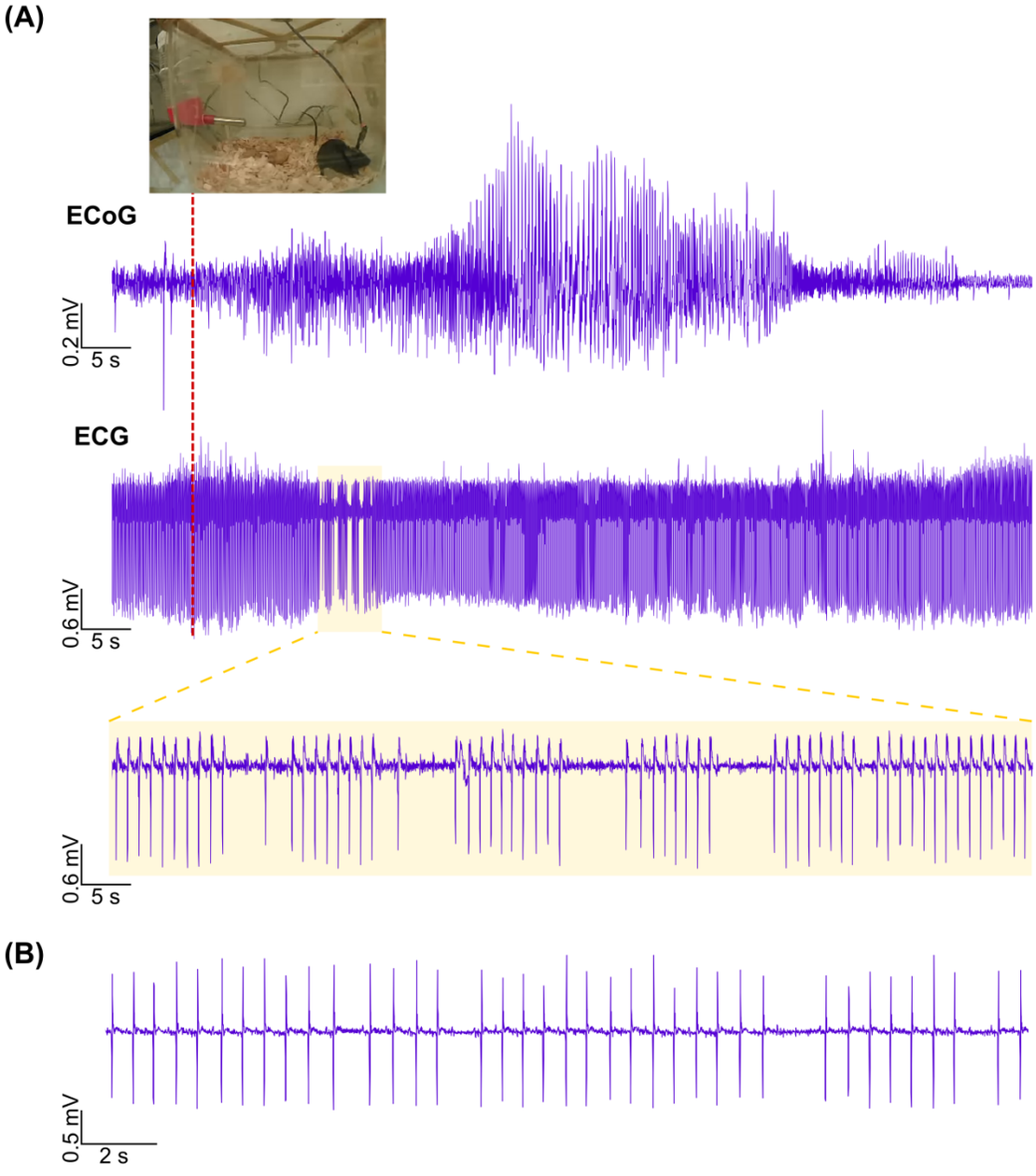

Figure S5: Arrhythmias observed during a non-terminal spontaneous seizure and at baseline in a *Hcn1*$^{M294L/+}$/*Kcnh2*$^{+/-}$ mouse. (A) ECoG and ECG traces of a spontaneous non-terminal seizure in a *Hcn1*$^{M294L/+}$/*Kcnh2*$^{+/-}$ mouse. Red dotted line marks the onset of a Racine 2-3 seizure, characterised by head nodding and forelimb clonus as depicted in the image. Yellow-highlighted section of the ECG trace indicates the presence of arrhythmias (variable AV block with irregular dropping of QRS complexes) which are shown in greater detail in the lower panel. **(B)** ECG trace showing baseline arrhythmias (bradyarrhythmia with AV block) in a separate untreated *Hcn1*$^{M294L/+}$/*Kcnh2*$^{+/-}$ mouse.

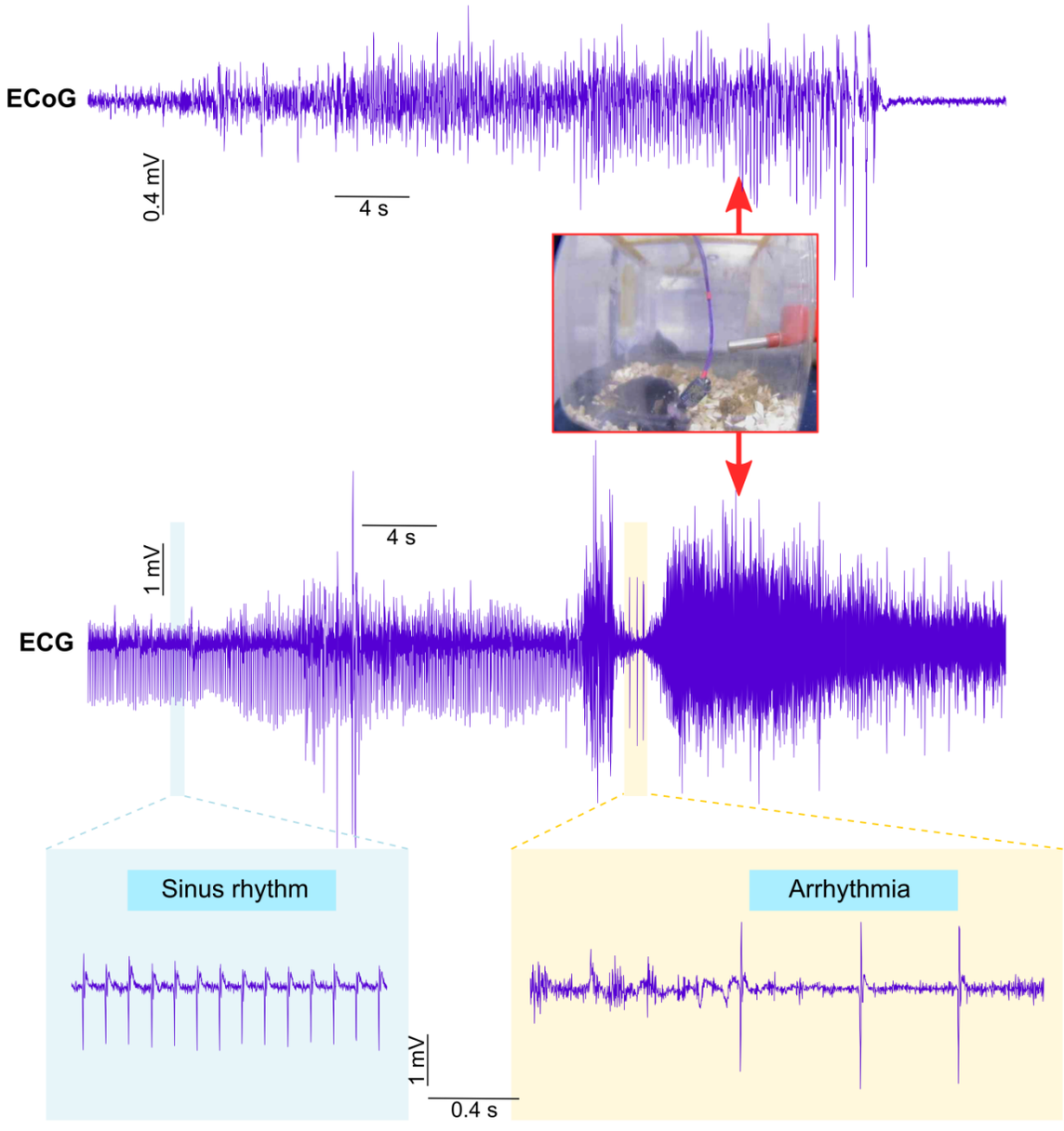

Figure S6: **ECoG and ECG traces of a spontaneous terminal seizure in a single *Hcn1*$^{M294L/+}$/*Kcnh2*$^{+/-}$ mouse**. Red arrows indicate where hind-limb extension occurs, also depicted in the inset image. Blue-highlighted region on the ECG trace shows sinus rhythm at the start of the seizure, while yellow-highlighted region shows the presence of cardiac dysfunction, including bradycardia with variable AV block, both of which are magnified in the lower panels.

Supplementary Videos

Video S1: Example video showing a non-terminal spontaneous Racine 4 seizure in a *Gabrg2*$^{R43Q/+}$/*Kcnh2*$^{+/-}$ mouse.

Video S2: Example video showing how a *Gabrg2*$^{R43Q/+}$/*Kcnh2*$^{+/-}$ mouse (left cage) progresses from a spontaneous Racine 2-3 (forelimb clonus, tail rearing) to Racine 4-5 (generalised tonic-clonic, jumping) seizure, resulting in hind-limb extension and death.

Video S3: Example video showing a *Hcn1*$^{M294L/+}$/*Kcnh2*$^{+/-}$ mouse experiencing hind-limb extension and terminal spontaneous seizure.

Video S4: Representative video of a *Hcn1*$^{M294L/+}$/*Kcnh2*$^{+/-}$ mouse undergoing a spontaneous Racine stage 2-3 seizure, with post-ictal EEG suppression observed following the seizure.

Supplementary Tables

Atenolol rescues premature mortality in genetic mouse models of sudden unexpected death in epilepsy.

Ming S. Soh[1], Amanda Hu[1], Alibek Kuanyshbek[1], Erlina S. Mohamed Syazwan[1], Hian M. Lee[1], Chaseley E. McKenzie[1], A. Marie Phillips[1,2], Lauren E. Bleakley[1], Christopher Semsarian[3,4,5], Ingrid E. Scheffer[1,6,7,8], Samuel F. Berkovic[6], Christopher A. Reid[1]

Author affiliations:

[1]The Florey Institute of Neuroscience and Mental Health, University of Melbourne, Parkville, VIC, Australia

[2]School of Biosciences, University of Melbourne, Melbourne, VIC, Australia

[3]Agnes Ginges Centre for Molecular Cardiology at Centenary Institute, The University of Sydney, Sydney, NSW, Australia

[4]Faculty of Medicine and Health, The University of Sydney, NSW, Australia

[5]Department of Cardiology, Royal Prince Alfred Hospital, Sydney, NSW, Australia

[6]Epilepsy Research Centre, Department of Medicine, University of Melbourne, Austin Health, Heidelberg, VIC, Australia

[7]Murdoch Children's Research Institute, The Royal Children's Hospital, Parkville, VIC, Australia

[8]Department of Paediatrics, University of Melbourne, Royal Children's Hospital, VIC, Australia

Supplementary Tables

Table S1- Summary of weight, ECoG and ECG comparison between the four genotypes from the *Gabrg2*$^{R43Q/+}$ and *Kcnh2*$^{+/-}$ cross

Weight (g)				
	Wild-type (*N*=45)	*Gabrg2*$^{R43Q/+}$ (*N*=41)	*Kcnh2*$^{+/-}$ (*N*=37)	*Gabrg2*$^{R43Q/+}$/ *Kcnh2*$^{+/-}$ (*N*=38)
P23-40	15.59 ± 0.46	15.93 ± 0.68	16.43 ± 0.69	16.10 ± 0.55
P40-60	20.07 ± 0.55	20.28 ± 0.61	21.38 ± 0.54	20.48 ± 0.23
P60-80	23.17 ± 0.48	21.40 ± 0.70	22.87 ± 0.58	21.83 ± 0.36
P80-100	24.22 ± 0.87	25.19 ± 0.99	26.34 ± 0.33	25.15 ± 0.80
Heart weight: body weight ratio (mg/g)				
	Wild-type (*N*=10)	*Gabrg2*$^{R43Q/+}$ (*N*=6)	*Kcnh2*$^{+/-}$ (*N*=10)	*Gabrg2*$^{R43Q/+}$/ *Kcnh2*$^{+/-}$ (*N*=6)
P70-80	7.59 ± 0.47	7.71 ± 0.31	7.52 ± 0.28	7.21 ± 0.42
ECoG parameters				
	Wild-type (*N*=10)	*Gabrg2*$^{R43Q/+}$ (*N*=13)	*Kcnh2*$^{+/-}$ (*N*=10)	*Gabrg2*$^{R43Q/+}$/ *Kcnh2*$^{+/-}$ (*N*=12)
Number of spikes per hour	0.06 ± 0.04***, ***	9.42 ± 1.96***, ****	0.05 ± 0.05****, ***	8.20 ± 1.68***, ***
Number of spike-wave discharges per hour	0.37 ± 0.14**, **	12.75 ± 3.25**, **	0.47 ± 0.22**, **	11.05 ± 3.87**, **
Number of spontaneous seizures	0.00 ± 0.00	1.08 ± 0.67	0.00 ± 0.00	1.00 ± 1.00
ECG parameters				
	Wild-type (*N*=6)	*Gabrg2*$^{R43Q/+}$ (*N*=5)	*Kcnh2*$^{+/-}$ (*N*=5)	*Gabrg2*$^{R43Q/+}$/ *Kcnh2*$^{+/-}$ (*N*=6)
Heart rate variability (RMSSD, ms)	2.00 ± 0.10	3.92 ± 0.80	3.90 ± 0.71	4.09 ± 0.99
P-wave duration (ms)	12.11 ± 0.14	12.14 ± 0.16	12.15 ± 0.17	11.95 ± 0.16
PR interval (ms)	35.27 ± 0.22	35.26 ± 0.22	35.7 ± 0.29	35.05 ± 0.25
QRS interval (ms)	13.55 ± 0.11	13.22 ± 0.13	13.40 ± 0.17	13.48 ± 0.13

RR interval (ms)	107.50 ± 0.94	108.3 ± 1.42	107.4 ± 1.56	105.6 ± 1.27
QT interval (ms)	41.38 ± 0.84****, ****	40.88 ± 0.37****, ****	46.48 ± 0.76****, ****	46.44 ± 0.43****, ****
QTc interval (ms)	39.77 ± 0.67****, ****	39.37 ± 0.32****, ****	44.42 ± 0.87****	44.96 ± 0.56****

Note: Data presented as mean ± SEM. Mixed model ANOVA with Tukey's multiple comparison was used for weights and ECG parameters; Kruskal-Wallis test with Dunn's post-hoc was used for ECoG parameters and Root Mean Square of Successive Differences (RMSSD); One-way ANOVA with Dunnett's was used for heart weight: body weight ratio.

Statistical comparison with wild-type:

** $P < 0.01$

*** $P < 0.001$

**** $P < 0.0001$

Statistical comparison with *Gabrg2*$^{R43Q/+}$:

** $P < 0.01$

*** $P < 0.001$

**** $P < 0.0001$

Statistical comparison with *Kcnh2*$^{+/-}$:

** $P < 0.01$

*** $P < 0.001$

**** $P < 0.0001$

Statistical comparison with *Gabrg2*$^{R43Q/+}$/ *Kcnh2*$^{+/-}$:

** $P < 0.01$

*** $P < 0.001$

**** $P < 0.0001$

Table S2- Summary of ECoG and ECG comparison between untreated and atenolol-treated *Gabrg2*$^{R43Q/+}$/*Kcnh2*$^{+/-}$ mice

ECoG parameters		
	Untreated (*N*=7)	0.6 g/L atenolol (*N*=6)
Number of spikes per hour	7.06 ± 2.19	8.23 ± 2.38
Number of spike-wave discharges per hour	9.89 ± 2.52	8.17 ± 2.96
Number of spontaneous seizures	0.00 ± 0.00	0.17 ± 0.17
ECG parameters		
	Untreated (*N*=7)	0.6 g/L atenolol (*N*=6)
RMSSD (ms)	2.32 ± 0.43	6.29 ± 1.16**
SDNN (ms)	4.82 ± 1.38	8.70 ± 2.65
P-wave duration (ms)	12.05 ± 0.11	11.95 ± 0.14
PR interval (ms)	34.98 ± 0.18	35.20 ± 0.22
QRS interval (ms)	13.44 ± 0.10	13.22 ± 0.13
RR interval (ms)	105.00 ± 0.98	120.50 ± 1.15****
QT interval (ms)	46.07 ± 0.35	47.28 ± 0.37*
QTc interval (ms)	44.79 ± 0.44	43.20 ± 0.37*

Note: Data presented as mean ± SEM. Mann-Whitney U-test was used for ECoG parameters, RMSSD and Standard Deviation of NN intervals (SDNN); Mixed model ANOVA was used for the remaining ECG parameters.

* $P < 0.05$

** $P < 0.01$

**** $P < 0.0001$

Table S3- Summary of weight, ECoG and ECG comparison between the four genotypes from the *Hcn1*$^{M294L/+}$ and *Kcnh2*$^{+/-}$ cross

Weight (g)				
	Wild-type (*N*=31)	*Hcn1*$^{M294L/+}$ (*N*=24)	*Kcnh2*$^{+/-}$ (*N*=28)	*Hcn1*$^{M294L/+}$/ *Kcnh2*$^{+/-}$ (*N*=24)
P23-40	14.26 ± 0.80*	10.20 ± 0.46*, **	14.02 ± 0.60**, **	11.32 ± 0.49**
P40-60	21.65 ± 2.76	19.12 ± 0.52	21.13 ± 0.58	18.73 ± 0.53
P60-80	25.01 ± 3.49*, *	22.06 ± 3.62*, *	24.45 ± 3.50*, *	22.06 ± 3.61*, *
P80-100	26.46 ± 0.62*, *	23.57 ± 0.56*	26.26 ± 0.92	24.07 ± 0.45*
ECoG parameters				
	Wild-type (*N*=10)	*Hcn1*$^{M294L/+}$ (*N*=12)	*Kcnh2*$^{+/-}$ (*N*=8)	*Hcn1*$^{M294L/+}$/ *Kcnh2*$^{+/-}$ (*N*=11)
Number of spikes per hour	0.025 ± 0.02***, **	34.88 ± 12.00***, **	0.00 ± 0.00**, **	28.84 ± 11.73**, **
Number of spike-wave discharges per hour	0.00 ± 0.00	0.01 ± 0.01	0.00 ± 0.00	0.02 ± 0.01
Number of spontaneous seizures	0.00 ± 0.00**	0.73 ± 0.47	0.00 ± 0.00**	1.55 ± 0.61**, **
ECG parameters				
	Wild-type (*N*=8)	*Hcn1*$^{M294L/+}$ (*N*=12)	*Kcnh2*$^{+/-}$ (*N*=6)	*Hcn1*$^{M294L/+}$/ *Kcnh2*$^{+/-}$ (*N*=10)
RMSSD (ms)	5.56 ± 0.62***, **	2.90 ± 0.34***, ****	8.04 ± 1.13****, ****	2.87 ± 0.18**, ****
P-wave duration (ms)	11.61 ± 0.04	11.70 ± 0.03	11.48 ± 0.05	11.53 ± 0.04
PR interval (ms)	33.02 ± 0.05	32.90 ± 0.04	32.86 ± 0.05	33.08 ± 0.05
QRS interval (ms)	13.53 ± 0.05	13.53 ± 0.04	13.54 ± 0.05	13.55 ± 0.04
RR interval (ms)	116.4 ± 0.61***, ***	94.25 ± 0.32***, ***	115.3 ± 0.78***, ***	94.31 ± 0.29***, ***
QT interval (ms)	36.08 ± 0.15***, ***, ***	37.54 ± 0.12***, ***, ***	43.23 ± 0.25***, ***, ***	39.04 ± 0.18***, ***, ***
QTc interval (ms)	33.69 ± 0.16***, ***, ***	38.81 ± 0.13***, ***, ***	40.69 ± 0.31***, ***	40.26 ± 0.16***, ***

Note: Data presented as mean ± SEM. Mixed model ANOVA with Tukey's multiple comparison was used for weights and ECG parameters; Kruskal-Wallis test with Dunn's post-hoc was used for ECoG parameters and RMSSD.

Statistical comparison with wild-type:

* $P < 0.05$

** $P < 0.01$

*** $P < 0.001$

Statistical comparison with *Hcn1*$^{M294L/+}$:

* $P < 0.05$

** $P < 0.01$

*** $P < 0.001$

Statistical comparison with *Kcnh2*$^{+/-}$:

* $P < 0.05$

** $P < 0.01$

*** $P < 0.001$

**** $P < 0.0001$

Statistical comparison with *Hcn1*$^{M294L/+}$/ *Kcnh2*$^{+/-}$:

* $P < 0.05$

** $P < 0.01$

*** $P < 0.001$

**** $P < 0.0001$

Table S4- Comparison of ECoG and ECG parameters between baseline and during a spontaneous seizure in untreated and atenolol-treated *Hcn1*$^{M294L/+}$/*Kcnh2*$^{+/-}$ mice.

ECoG parameters		
	Untreated (*N*=6)	0.6 g/L atenolol (*N*=3)
Number of spikes per hour	24.32 ± 9.20	11.86 ± 9.07
Number of spike-wave discharges per hour	0.02 ± 0.01	0.22 ± 0.20
Number of spontaneous seizures	2.33 ± 0.49	2.33 ± 0.88

ECG parameters				
	Untreated (N=6)		0.6 g/L atenolol (N=3)	
	Baseline	Seizure	Baseline	Seizure
RMSSD (ms)	2.80 ± 0.25	1.87 ± 0.11****	3.32 ± 0.15****, ****	2.18 ± 0.16****, ***
SDNN (ms)	2.71 ± 0.25	1.40 ± 0.11**	4.74 ± 0.20**	1.41 ± 0.12**
P-wave duration (ms)	11.52 ± 0.04	N/A	11.64 ± 0.06	N/A
PR interval (ms)	33.86 ± 0.08	N/A	33.99 ± 0.09	N/A
QRS interval (ms)	13.37 ± 0.05	13.34 ± 0.05	13.16 ± 0.05	13.40 ± 0.07
RR interval (ms)	96.18 ± 0.42	81.65 ± 0.19***	115.9 ± 0.56***, ***	96.52 ± 0.56***, ***
QT interval (ms)	38.80 ± 0.21	39.79 ± 0.24**	38.39 ± 0.20***	40.54 ± 0.17***, ***
QTc interval (ms)	39.18 ± 0.20	43.75 ± 0.26***	35.71 ± 0.17***, ***	41.38 ± 0.21***, ***, ***

Note: For ECG; Mixed model ANOVA with Tukey's multiple comparison was made between baseline and seizure within respective treatment group and between untreated and atenolol-treated groups for all except RMSSD and SDNN, which were analysed with paired t-test (baseline-seizure comparison) or Kruskal-Wallis with Dunn's posthoc (treated vs untreated). For ECoG; Mann-Whitney test. Data presented as mean ± SEM.

Respective baseline-seizure comparison:

** $P < 0.01$

*** $P < 0.001$

**** $P < 0.0001$

Comparison between untreated baseline and atenolol-treated groups:

*** $P < 0.001$

**** $P < 0.0001$

Comparison between untreated seizure and atenolol-treated groups:

** $P < 0.01$

*** $P < 0.001$

**** $P < 0.0001$

N/A Not available: Measurement was not possible due to signal interference during the seizure.